JPhys Energy

PERSPECTIVE • OPEN ACCESS

Recent progress in encapsulation strategies to enhance the stability of organometal halide perovskite solar cells

IOP Publishing J. Phys. Energy 2 (2020) 031002 https://doi.org/10.1088/2515-7655/ab8774

Journal of Physics: Energy

PERSPECTIVE

Recent progress in encapsulation strategies to enhance the stability of organometal halide perovskite solar cells

Francesca Corsini and Gianmarco Griffini[1]

Department of Chemistry, Materials and Chemical Engineering 'Giulio Natta', Politecnico di Milano, Piazza Leonardo da Vinci 32, Milano 20133, Italy

[1] Author to whom any correspondence should be addressed.

E-mail: gianmarco.griffini@polimi.it

OPEN ACCESS

RECEIVED
31 January 2020

REVISED
25 March 2020

ACCEPTED FOR PUBLICATION
7 April 2020

PUBLISHED
3 July 2020

Abstract

Organometal halide perovskite solar cells (PSCs) have emerged as promising candidates for next-generation thin-film solar cells. Over the past ten years, the efficiency of PSCs has increased from 3.8% to over 25% through the optimization of the perovskite film formulation and the engineering of suitable fabrication strategies and device architectures. However, the relatively poor long-term device stability, which has not been able to exceed some hundreds of hours until now, represents one of the key aspects still hampering their widespread diffusion to commercial contexts.

After briefly introducing the origin and basic mechanisms behind PSC degradation and performance decline, a systematic outline and classification of the available strategies to improve the long-term stability of this class of photovoltaic devices will be presented, mainly focusing on encapsulation procedures. Indeed, the aim of this review is to offer an in-depth and updated account of the existing encapsulation methods for PSCs according to the present understanding of reliability issues. More specifically, an analysis of currently available encapsulation materials and on their role in limiting the penetration of UV light and external agents, such as water vapour and oxygen, will be proposed. In addition, a thorough discussion on various encapsulation techniques and configurations will be presented, highlighting specific strengths and limitations of the different approaches. Finally, possible routes for future research to enhance the effectiveness of the most performing encapsulation procedures will be suggested and new paths to be explored for further improvements in the field will be proposed.

1. Introduction

Organometal halide perovskite solar cells (PSCs) are photovoltaic (PV) devices incorporating a perovskite-structured compound with generic chemical formula ABX_3 as light-harvesting active layer. In this area, methyl-ammonium-lead-iodide ($MAPbI_3$) is to date the most commonly used and studied material platform for use as light absorber in such devices. At present, high power conversion efficiencies (PCEs) of over 21% have been reported with this system [1], which is however prone to pronounced thermal and moisture instability [2–6]. In this regard, efforts in this field have been focused on composition engineering of hybrid perovskites to pursue a more performing and more stable system for PV applications. Notably, the present tendency is to replace $MAPbI_3$ with formamidinium-lead-iodide ($FAPbI_3$) [7–9] or other potential absorbers such as Caesium-formamidinium-lead-halide perovskites [10–12] and triple-cation perovskites [13–15]. Within this framework, tuning the composition and relative concentration of organic cations or halide anions in perovskite compounds is currently a largely established strategy [9, 16–18]. Indeed, the best performing PSCs are to-date lead-based (that is B = Pb) and are composed of mixtures of methylammonium $CH_3NH_3^+$ (MA), formamidinium $HC(NH_2)_2^+$ (FA), Rubidium Rb^+ (Rb) and/or Caesium Cs^+ (Cs) monovalent cations on the A site and iodide I^-, chloride Cl^- and/or bromide Br^- monovalent halogen anions on the X site, $FA_{1-x-y-z}MA_zCs_yRb_xPb(I_{1-x-y}Br_xCl_y)_3$ [19–22]. These compounds have been demonstrated to enable a black tetragonal photoactive perovskite phase featuring enhanced thermal and photo stability [23]. Alternatively, the design of 2D, 1D and 0D layered perovskite materials has

recently been considered as a promising option to fabricate perovskite compounds characterized by improved stability [16, 24–32].

Recently, PSCs have been identified as promising candidates for next-generation thin-film solar cells. The prospective low material costs, ease of processability [33] and excellent photon energy utilisation, that approaches the values of state-of-the-art technologies (such as GaAs) [34], make PSCs a viable and potentially cost-effective alternative to some consolidated, existing PV technologies [35, 36].

Research in the field of PSC materials and devices in the past decade have led to an impressive increase in their PCE, through the development of novel perovskite formulations, the engineering of suitable interface materials and fabrication procedures, and the progress in advanced device architectures. Since 2009 [37], their PCE has grown from 3.8% to 25.2% [38], now exceeding the performance of conventional thin-film solar cells such as copper-indium-gallium-selenide (CIGS) solar cells (23.4%), and approaching that of monocrystalline silicon solar cells (26.1% for single-junction silicon cells without concentrators) [39].

In spite of these notable advancements, the severe instability of PSCs to environmental factors (moisture, UV light, oxygen, and temperature) represents one of the most critical factors currently hampering their widespread commercialization. Indeed, under ambient conditions PSCs undergo significant morphological and structural changes, optical absorption decay, and deterioration of the opto-electronic properties, which negatively affect their PV performance [4, 40–43].

For what concerns moisture, as demonstrated in previous reports [44–46], due to the inherent hygroscopic nature of the organic cation, in the presence of water perovskites tend to hydrolyse back to their precursors. Specifically, water can penetrate the perovskite lattice to form mono and dihydrated perovskite phases in which the organic cations are no longer strongly bonded to the I^- of the inorganic octahedra, but they interact through hydrogen bonding with water molecules forming water-cation chains. As a result, the phase segregation of PbI_2 crystals takes place, too. Moreover, as proposed by Walsh *et al* [47], water can also deprotonate the methylammonium cation, breaking bonds between the A site and the lead halide octahedra to produce methylamine, while it can protonate any excess iodide to form hydriodic acid. Both of these compounds are highly volatile at room temperature. Consequently, in an open system, the continuous release of these gases can drive the decomposition reaction forward and completely degrade the perovskite layer.

Oxygen molecules can also cause the decomposition of perovskite materials, if the latter is exposed to light and dry air. In fact, the combination of molecular oxygen and light leads to a photo-oxidation process, where a photoexcited electron in the conduction band of the perovskite reacts with molecular oxygen to form superoxide (O_2^-). These superoxide anions can then initiate the decomposition of perovskite by deprotonation reaction with organic cations, yielding the formation of lead iodide PbI_2, iodine, water molecule and methylamine gas [48, 49].

In addition, most perovskites cannot endure high temperature (i.e. temperature higher than 130 °C–170 °C depending on the perovskite composition) due to the generation of thermal stresses provoked by the phase transition of their crystalline structure upon heating [26, 50, 51]. As reported by Conings and coworkers [52], these thermal stresses can induce the degradation of the perovskite active layer, leading to the evolution of volatile organic species and to segregation of PbI_2 and even of some metallic $Pb_{(0)}$ clusters. This process is greatly accelerated in the presence of either oxygen or water, which interact with the organic part of the structure via complex formation and hydrogen bonding, ultimately disrupting the perovskite crystal lattice and reducing the attraction between inorganic octahedra and the organic cations, as previously described [46, 53]. Moreover, PSC devices can significantly degrade even in inert atmosphere while heating to temperatures comparable to the higher range of operational temperatures in full sunlight (∼85 °C). In this case, the decomposition occurs due to thermal instability of their organic constituents, mainly the 2,2′,7,7′-Tetrakis[N,N-di(4-methoxyphenyl)amino]-9,9′-spirobifluorene (spiro-OMeTAD) hole transport layer (HTL) [54, 55].

Finally, continuous UV light irradiation causes non-stoichiometry induced defects in some types of electron transport layers (ETLs), e.g. in mesoporous/planar TiO_2, and the consequent compromise of the device performances. Specifically, as firstly studied by Snaith's group [56], UV excitation is responsible for the creation of a large density of deep trap sites in the meso-TiO_2 for the injected electrons, which leads to performance decline upon continuous exposure.

Considering this discussion and the present understanding of the degradation mechanisms of perovskite materials and devices, improving the long-term stability of PSCs represents one of the most urgent and crucial issues faced by this field at present. The current strategies to prevent degradation and enhance device lifetime fall into two broad categories [57]:

(a) intrinsic approaches, which explore the possibility to reduce the innate vulnerabilities of perovskite materials by modifying formulation stoichiometry and composition, so as to achieve inherently more stable crystal structures [6, 9, 46, 58] (e.g. low-dimensional-networked perovskites [27, 32, 59, 60]), by

selecting appropriate manufacturing techniques [61, 62], by employing highly-performing HTLs and ETLs [63–65], by properly engineering interfaces [57, 66, 67] and by incorporating suitable buffer layers between the perovskite film and HTL or ETL [68].

(b) extrinsic approaches, which allow to enhance the stability of PSCs through appropriate encapsulation methods, and rely on the application of materials and structures characterized by high barrier performance towards moisture, oxygen, UV light and temperature, ultimately resulting in the protection of the cathode interface and the active layer from deterioration [46, 69].

This perspective aims to summarize the extensive progress made in the area of PSC stabilization, specifically focusing on the use of encapsulation as versatile protective strategy operating on the complete PSC device. More specifically, we will provide an overview of the encapsulation materials and routes that have been explored to date, highlighting the strengths and the weaknesses of the presented approaches, and providing possible guidelines for future research in this important field.

2. Encapsulation requirements

Encapsulation has been demonstrated to play a fundamental role in avoiding degradation or improving stability for a number of different PV technologies [20, 70–75]. Thus, it is considered as a promising way to circumvent instability issues in the case of PSCs as well [69]. If properly designed, encapsulation films or coatings can act as barrier layers limiting the diffusion of oxygen and moisture, preventing the penetration of UV light, reducing the sensitivity to sharp thermal fluctuations and also inhibiting the irreversible escape of volatile decomposition products possibly forming from the perovskite materials, ultimately resulting in the protection of the electrode interface and the active layer [70].

High-performance encapsulation materials should possess good processability, excellent chemical inertness and high barrier performance for oxygen and moisture, which means reasonably low water and oxygen absorptivity and permeability [76]. In this context, two reference figures of merit are the oxygen transmission rate (OTR) and the water vapour transmission rate (WVTR) which must be in the order of 10^{-4}–10^{-6} cm^3 $m^{-2}d^{-1}$ atm^{-1} and 10^{-3}–10^{-6} $gm^{-2}d^{-1}$, respectively, in order to guarantee optimum encapsulation performance [77]. Indeed, the barrier performance of encapsulant materials strongly affects the lifetime of PSC devices. In particular, the rate of PCE decline for the encapsulated PSCs has been demonstrated to depend on the WVTR of the barrier-sealant system according to the following empirical expression [78]:

$$DR[\%d^{-1}] = \frac{DR_{max} \cdot WVTR^{n}}{(WVTR_{50})^{n} + WVTR^{n}}$$

where DR stands for PCE degradation rate of the PSC device, DR_{max} for the maximum DR (corresponding to the PCE DR gauged for the unencapsulated sample), $WVTR_{50}$ for the WVTR value when DR is 50% of DR_{max}, and n is the coefficient of this Hill function controlling the sigmoidicity of curve. This relationship is extremely useful to design new high performing encapsulation barriers and sealant systems and to predict their degradation rate in dark conditions and at room temperature and ambient humidity. However, it must be pointed out that this is an empirical expression valid only under given encapsulation and testing conditions (that is, those used to build this expression). To assess the influence of the performance of barriers on the lifetime of the PSCs under different encapsulation setups (i.e. edge sealing), PSC architectures (i.e. inverted p-i-n structure) and test conditions (i.e. different temperatures, humidity and irradiation), and therefore to extract phenomenological relations between the two rates in different settings, further systematic studies on WVTRs of encapsulation systems and on degradation of packaged PSCs over time are required.

Moreover, encapsulants should display total light transmission (>90% of incident light), relatively high dielectric constant to mitigate potential-induced-degradation (PID) and excellent resistance to UV degradation and thermal oxidation. Finally, other important features are good mechanical strength, excellent adhesion to the PSC module to minimize the risk of delamination, coefficients of thermal expansion close to that of PSC components to avoid mechanical damage during stability tests, and high flexibility to absorb any fluctuation in strain energy during bending or temperature cycling [69, 79].

Technological requirements for highly effective encapsulations must also be considered. In particular, the cleanness of PSC edges from residual perovskite materials is an essential step in encapsulation procedures to avoid the formation of preferential routes for water and oxygen penetration and early degradation, as well as to favour side leakage protection and edge sealing. To this end, prior to PSC modules encapsulation, edge cleaning is recommended, usually by means of mixtures of chlorobenzene and N,N-dimethylformamide [80, 81] or of toluene and ethanol [82]. Alternatively, scratching away the residual materials with a razor blade and then wiping with proper solvents has been proven successful [82]. During this operation, it is imperative

to work in inert atmosphere or at least to keep the exposure time of perovskite layer to air below 10 min so as to minimize its degradation. It is worth noticing that cleaning the PSC edges is crucial to hinder premature degradation. However, only proper edge encapsulation systems can effectively extend the long-term stability of perovskite devices. Indeed, in comparison to fully encapsulated devices with a protected edge, partially encapsulated modules (i.e. without edge sealing) were shown to yield shorter lifetime [43, 82–84].

Finally, along with the specific material and technological requirements discussed above, another key factor for reliable and effective encapsulation is the selection of a suitable pattering strategy. In particular, the encapsulation pattern must be designed not to cause any thermal and/or photochemical damage to the PSCs, to prevent side-penetration of water vapor/oxygen, and to guarantee long-term stable adhesion to the PSC module in harsh weathering conditions. Within this context, typical packaging systems can be divided into two major categories: top encapsulant barriers, in which a thin protective layer is deposited on top of the module; edge sealing, in which the sealant is placed around the device and it is bonded to a cover substrate. The latter approach is usually more reliable for stability tests since it enables the suppression of side penetration effects. Even better, blanket encapsulation patterns, which include both cover barrier and edge sealing, have been demonstrated to create a pressure-tight environment that not only blocks the ingress of external moisture but also prevents the escape of any volatile materials from the PSC. For this reason, these strategies are considered to be the most effective and reliable for long-term, stable packaging of PSCs [12, 83–87].

3. Methods to assess the encapsulation performance and the stability of packaged PSCs

Improving the long-term stability of PSCs through device encapsulation may represent one of the cornerstones for their straightforward deployment on the market. Despite the great efforts made by the research community in this field, in many cases publications dealing with the evaluation of the stability of PSC materials and devices lack consistency in the adopted experimental procedures and in the used stress factors. It is therefore challenging to replicate and compare results from lab to lab, and not immediate to be able to gain a deep understanding of the degradation processes described in different research works. In the attempt to overcome this issue, standardized testing protocols have been recently proposed to assess the long-term performance of PSCs and estimate the effectiveness of different encapsulation methodologies under given testing conditions, with the aim of achieving consistent and reproducible results in the field [88, 89].

The most relevant standards for testing the long-term stability of PV cells, issued by the International Electrotechnical Commission (IEC) and the International Summit on Organic Photovoltaic Stability (ISOS), are summarized in the so-called IEC 61215 norm [90] and ISOS protocol (89). These documents summarize different possible stress tests for the evaluation of the stability of inorganic, hybrid and organic PVs and regulate the conditions to perform accelerated-aging/weathering tests. A list of accelerated ageing tests widely encountered in current publications in the field include: damp heat test, thermal cycling test, outdoor exposure test and light soaking tests.

In damp heat test, exposure to humidity on a long-time scale is tested. To this end, the PSC assembly is maintained at 85 ± 2 °C and RH of 85 ± 5% for 1000–1048 h, followed by a recovery time of 2–4 h at 23 ± 5 °C and RH <75%. In thermal cycling tests, PSCs are cycled between 50 and 200 times from −40 to 85 °C with at least a dwell time of 10 min. During the cycles, the heating and cooling rates should be between 45 and 100 °C h^{-1}, whereas the time for one cycle should not be exceed 6 h. A continuous current could be applied to the device during each heating step. Then, a recovery time of at least 1 h at 23 ± 5 °C and RH < 75% is allowed. Degradation processes which do not occur under laboratory conditions are revealed performing a standardized outdoor exposure test. The preliminary resilience to outdoor conditions is tested by mounting the PSC normal to the local latitude ± 5° so that the device is exposed to at least 60 kW h m^{-2}, and by connecting the module to a resistive load or a maximum power point (MPP) tracker. The test outcome is the time (expressed in days) after which encapsulated devices reach 80% of their initial efficiency (T_{80}). Light soaking tests allow to investigate the chemical-physical modifications occurring to the extraction layers as a result of continuous illumination. In these conditions, the device is placed under a 100 mW cm^{-2} irradiance (using an AM 1.5 G filter) for 1000 h and constant temperature in the presence of a resistive load. During the test, devices are maintained at their MPP using a MPP tracking algorithm. A set of three J–V curves, that is, in the dark, at 10 mW cm^{-2}, and at 100 mW cm^{-2} light intensity are then automatically collected at fixed time intervals, and the device performance is evaluated in time.

In addition to such standardized approaches for the evaluation of device stability in different operating conditions, other methodologies are currently in place to assess the efficiency of the encapsulation layer. Among these, the so-called Calcium test [85, 91, 92] can be performed to directly examine the performance of the encapsulant material as effective moisture barrier. Through simple optical measurements, this test

enables to evaluate the transport rate of moisture through the packaging layer and to quantitatively monitor moisture ingress in a sealed system, by monitoring the transition from opaque to transparent of a thin (<100 nm) Ca layer thermally evaporated on top of the PSC device prior to encapsulation. Indeed, in the presence of moisture, thin layers of metallic calcium immediately become transparent, indicating its reaction with water. Calcium test is usually performed at 65 °C/85% RH or in combination with standardized accelerated tests (e.g. damp heat and thermal cycling).

Finally, the ability of a specific encapsulation material to limit or prevent the degradation of the perovskite layer as a result of the interaction with water, oxygen, light or/and combinations thereof can be assessed using RGB (red, green, blue) colour measurements. This is a relatively simple technique which gives a clear indication of the perovskite degradation pathway and the impact of various encapsulants on degradation rate. More specifically, using time-lapse photography, this approach allows to track Pb-based perovskite layer degradation to lead iodide (PbI_2) and thus provide a qualitative estimate of the efficacy/reliability of a given encapsulation procedure and material [80, 93, 94].

4. Encapsulation strategies

To date, various encapsulation methods have been developed for PSCs. One of the most widespread approaches is based on glass–glass encapsulation, where the PCS device is sandwiched between two glass sheets using thermo-curable (e.g. ethylene vinyl acetate (EVA) [12], Surlyn ionomer [5], butyl rubber and polyisobutylene (PIB) [85, 95]) or UV-curable sealants (such as Ossila E132 resin [96], epoxy resin by ThreeBond [84], Vitralit epoxy glue by Panacol [97]). Also, edge sealants (mainly butyl rubber and PIB [85] or UV epoxy adhesives [97]) should be applied for preventing, or at least delay, moisture and oxygen ingress from the lateral perimeter, thus extending the lifetime of PSCs [82, 91]. This technique is very affordable, relatively straightforward, and extremely efficient since glass has the best water and oxygen blocking properties as transparent material. However, it is incompatible with flexible applications, the latter being a market that has dramatically grown in the last years [98, 99]. Hence, alternative methods in which rigid glass coverslips are replaced by flexible films have recently been developed [78, 100–102].

Among these, an encapsulation approach using ultra-thin flexible glass sheet has been very recently proposed. This emerging technique combines the excellent barrier properties typical of rigid glass coverslips with thin-film flexibility. In particular, flexible glass was shown to exhibit ultra-low WVTR values (i.e. $\sim 10^{-7}$ g m^2 d^{-1}), making it particularly suitable for use in optoelectronics. Nevertheless, further studies are required to reduce the high fabrication costs and to deepen the knowledge on the effect of this encapsulation process on PSC performance and on the long-term stability of packaged devices [100, 103].

Other more widely spread encapsulation approaches for flexible applications make use of polymeric laminates and thin-film barrier-coated polymer webs. These encapsulation strategies stood out for their versatility in terms of choice of polymeric materials (poly(methyl methacrylate) (PMMA) [80, 93, 104], polyethylene terephthalate (PET) [105], polytetrafluoroethylene (PTFE) [83, 106, 107], polycarbonate (PC) [80], polydimethylsiloxane (PDMS) [3], ethylene-vinyl alcohol copolymer (EVOH) [108], polyethylene naphthalate (PEN)), flexible polymer-based hybrid multilayers [78, 109–111] and polymer composites [104, 112, 113], i.e. polymeric matrices (e.g. PMMA, EVOH) in which fillers (such as graphene oxide (GO) or SiO_2 particles) are dispersed, and for the possibility of applying these barrier layers on various device substrates [83, 102]. Indeed, these films can be laminated on top of a device that is processed on a rigid glass substrate or metal/plastic foil, or they can be applied both as substrate and as encapsulating layer through roll-to-roll lamination to obtain flexible PSCs.

Currently, the most technologically promising, but also challenging, option is thin-film encapsulation (TFE). It consists in the direct deposition of a single protective flexible ultra-thin layer (i.e. Al_2O_3, SiO_x, SiN, TiO_2, Zn_2SnO_4, Parylene-C, ultrathin plasma polymeric film or organic-inorganic hybrid polymer layers [86, 114, 115]) or a multilayer stack, composed of multiple pairs of organic and inorganic layers called a dyad [116, 117], on top of perovskite devices using vacuum deposition techniques such as chemical or physical vapour deposition (CVD, PVD), plasma-enhanced chemical vapour deposition (PECVD), atomic layer deposition (ALD) and other vacuum coating techniques [102]. Notably, ALD has been proven to be particularly suitable for organic and flexible electronics, such as PSCs [35, 69, 118]. However, despite its effectiveness, ALD is an expensive approach since it requires high-cost vacuum-based equipment and processes, as well as a detailed understanding of the interaction between the deposition process, the barrier layer material, and the device structure. For this reason, its large-scale applicability is still hampered.

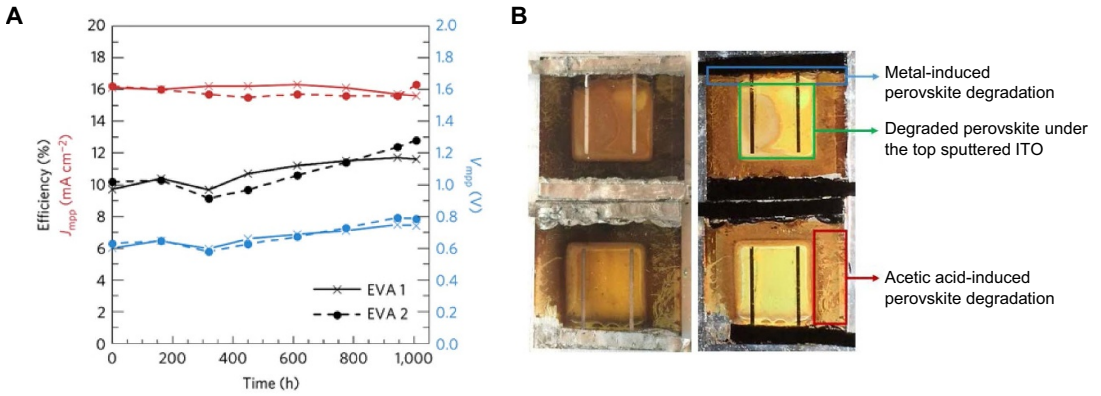

Figure 1. (A) Efficiency (black), J_{MPP} (red), and V_{MPP} (light blue) of a PSC encapsulated between two glass plates with EVA cover encapsulant and butyl rubber edge seal during (1000 h of continuous maximum-power-point tracking). Reprinted with permission from [12], Springer Nature, Copyright 2017. (B) Encapsulated PSCs after 1000 h of damp heat testing. Photos were taken both in indoor light (left) and under a solar lamp (right). The green box highlights perovskite degradation to PbI_2 since the active area turned from initial brown to yellow. Metal-induced degradation of the active area adjacent to the metal ribbon was observed (blue box). The presence of yellow lines outside the sputtered ITO again reveals degradation of perovskite into PbI_2, likely induced by acetic acid released from EVA cover encapsulant in damp heat conditions (red box). Reprinted with permission from [82], Royal Society of Chemistry, Copyright 2018.

5. Glass-glass encapsulation methods

Conventional PSC encapsulation methods are based on glass-glass packages, where two critical components are the cover encapsulant adhesive and the edge sealant. The cover encapsulant layer, which fills in excess volume in the package, holds the glass sheets tightly together with the PSC device and ensures that the edge sealant remains compressed throughout prolonged field exposure [82]. Instead, the edge sealant prevents the direct contact of the edges of the PSC device with the surrounding environment [119].

Different encapsulant adhesive and edge-seal materials have been proposed (table 1). Early approaches employed thermo-curable sealants such as EVA, Surlyn ionomer, butyl rubber and PIB.

EVA is by far the dominant encapsulant in the solar industry [120]. Recently, promising results in the use of EVA coated glass cover as an encapsulant have been provided by Bush *et al* [12]. They sandwiched a glass/ITO/NiO/$Cs_{0.17}FA_{0.83}Pb(Br_{0.17}I_{0.83})_3$/LiF/PCBM/$SnO_2$/ZTO/ITO/Ag device between two glass sheets with EVA and two sheets of 3-mm-thick glass edge-sealed by butyl rubber at a curing temperature of 140 °C for 20 min. As depicted in figure 1(A), the encapsulated device withstood the IEC 61215 [88] damp heat test (1000 h at 85 °C with 85% relative humidity) without any loss in PCE, thanks to the high barrier effect of this encapsulation architecture and the low elastic modulus of EVA and butyl rubber (10 and 9 MPa, respectively). While the latter result was encouraging, further studies [82] conducted on the same packaged device under accelerated conditions (120 °C–100% RH for 20 h) highlighted that it suffered from visible degradation that was accompanied by a noticeable drop in photocurrent. In particular, as it was already observed after damp heat test, in the EVA package, yellow lines outside of the ITO appeared (see figure 1(B)). This is a sign of the perovskite degrading into PbI_2, likely due to heat- and moisture-induced decomposition of the EVA into acetic acid [121] which in turn reacted with the perovskite active layer and the soda lime glass, causing PDI [122].

To overcome the limitations of EVA, ionomer-based Surlyn encapsulants have been proposed since not only they are characterized by a lower chemical reactivity with perovskite, but also they display better electrical insulation properties and a lower WVTR (0.66 g/(m^2 day) compared to 28 g/(m^2 day) of EVA [87]. For example, Burschka *et al* [5] tested the long-term stability of a glass/FTO/TiO_2/$CH_3NH_3PbI_3$/spiro-OMeTAD/Au device sealed using Surlyn 60 as an encapsulant. Surlyn sheets were melted under argon at 100 °C for 40 s using a hot press with a pressure equal to 0.4 bar. Subsequently, the impact of the sealing procedure on the performance of the cells was evaluated comparing the PCE values prior to (t = 0 h) and after the sealing process. A PCE decrease from 12.5% (unsealed PSC) to 8.2% (PSC sealed with Surlyn 60) was reported. A similar impact of this sealing procedure was also observed by Matteocci *et al* [84] where a remarkable decrease of the PCE value (32.4% of its initial value) was reported, mainly due to the decrease in short-circuit current density J_{sc} (16.4%) and fill-factor FF (13.7%). The adverse effect of encapsulation process itself on the performance of PSCs could be attributed to the heating process of the cell at the curing temperature (100 °C) of the thermoplastic encapsulant, owing to the poor intrinsic thermal stability of the organic spiro-OMeTAD HTL [50, 54], but also (marginally) to the perovskite active layer [46, 52, 53, 123]. In

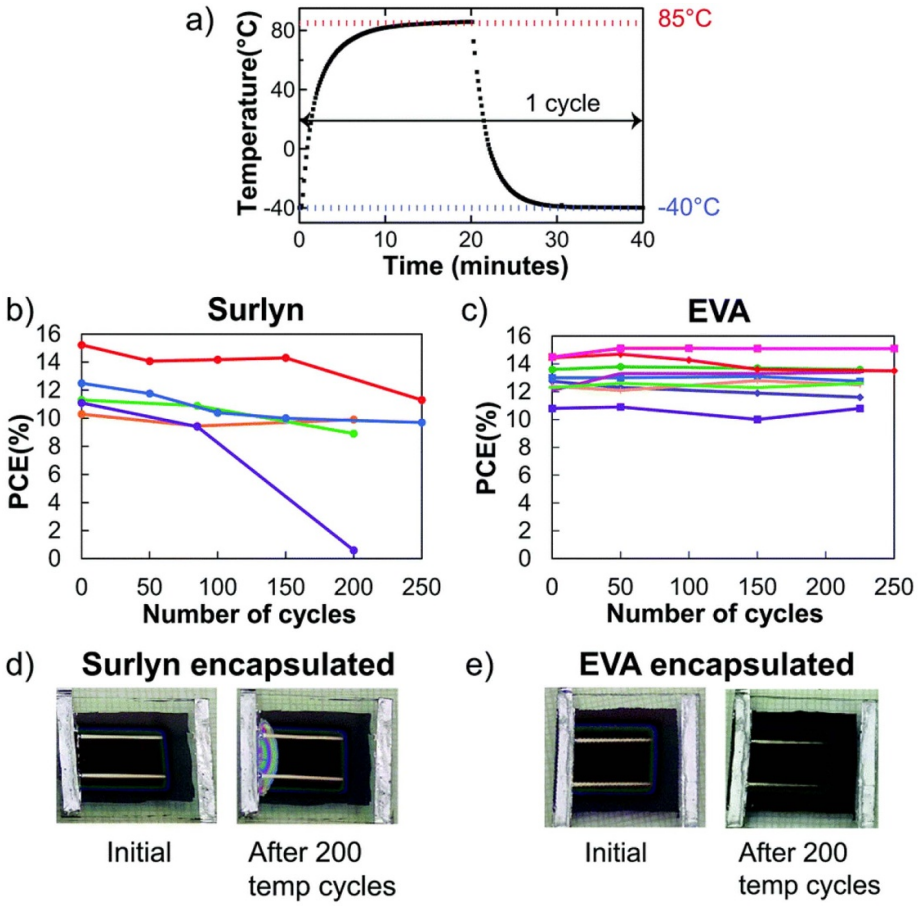

Figure 2. (A) Temperature profile imposed to glass-glass packaged PSCs during temperature cycling test. Evolution of PCE during temperature cycling of solar cells encapsulated with (B) Surlyn and with (C) EVA. Picture of the packaged PSCs using (D) Surlyn and (E) EVA before and after 200 temperature cycles. Reprinted with permission from [87], Royal Society of Chemistry, Copyright 2018.

fact, a PCE decrease of only 7.6% of its original value was obtained when the cell was sealed at room temperature applying a pressure of 0.4 bar. For what concerns the results of long-term light soaking at a light intensity of 100 mW cm^{-2} and a temperature of 45 °C, in these conditions the device was found to maintain more than 80% of its initial PCE after a period of 500 h. Also, no change in the short-circuit photocurrent was noticed, which indicates that there was no photodegradation of the perovskite light harvester layer. The decrease in PCE was therefore attributed to a decrease in both the open-circuit voltage (V_{oc}) and the FF, and the similar trend observed in the two decay processes suggests that their decrease is linked to a reduction in the shunt resistance [5]. Moreover, the PSCs packaged using Surlyn as encapsulant showed poor mechanical stability under the IEC 61215 temperature cycling test (see figure 2). The high elastic modulus of the Surlyn encapsulant (394 MPa) and the low fracture energy, which lead to delamination and to a drop in performance, factually limit the potentiality of Surlyn as successful encapsulant [87].

Conversely, very satisfactory outcomes have recently been achieved using polyolefin and butyl rubber as encapsulation materials, thus making them increasingly more popular within the thin film PV field. In particular, polyisobutylene (PIB) is probably one of the best candidates both as cover encapsulant layer [85] and edge sealant [12, 85, 91, 124] among those explored over the last two decades in the PV industry [95, 125] because of its low elastic modulus (9 MPa) and low WVTR (10^{-2}–10^{-3} g/(m^2 day)). Also, its high electrical resistivity (that makes it less prone to PID) and its low cost when compared to EVA, ionomer-based Syrlyn and UV-curable epoxies commonly used for encapsulating silicon solar modules are very attractive features [124, 126]. Furthermore, unlike EVA and UV-curable epoxies, PIB displays very poor chemical reactivity with perovskite, can be applied at a relatively lower temperature and does not require UV curing, making it a suitable encapsulation material for PSC modules.

In a recent work, Shi *et al* [85] demonstrated the effectiveness of using PIB as an edge sealant and encapsulant for glass/FTO/c-TiO_2/$FAPbI_3$/PTAA/Au PSCs. Three different methods were used to achieve glass-glass encapsulation of PSC devices, as shown in figure 3(A). Methods 1 and 2 used PIB in a conventional way as an edge seal, whereas in method 3, PIB blanketed the entire area underneath the cover glass, including

the perovskite and HTL layers, and the edge margins. The average PCE of PSCs immediately before and 1 d after encapsulation was found not to be significantly affected by any of the packaging processes. This result could be associated both to the lower curing temperature and to the higher thermal resistance of PTAA HTL and $FAPbI_3$ active layer compared to spiro-OMeTAD and $MAPbI_3$, respectively [13, 14, 54]. In order to evaluate the effectiveness of the three different sealing schemes, two accelerated lifetime tests, damp heat and thermal cycling, were performed in compliance with IEC 61215:2016. Among the three methods, blanket encapsulation using PIB showed superior stability results, allowing to effectively reduce moisture ingress in PSCs, to prevent the escape of volatile organic degradation products and to substantially improve their ability to withstand thermal fluctuations. Indeed, cells encapsulated through this method passed the thermal cycling test, by withstanding 200 cycles without degradation in cell performance, which is one the best result published to date. In addition, as reported in figure 3(B), these cells survived 540 h of damp-heat test. These noteworthy improvements were attributed to the much tighter sealing at the device edges and the ability of PIB blanket encapsulant to suppress the escape of gaseous decomposition products, inhibiting the perovskite decomposition reaction and the degradation of the HTL. Moreover, shelf life tests on PCSs encapsulated using UV-cured epoxy and EVA were also conducted to provide direct comparisons with PIB. The PCE of PSCs packaged with either EVA or UV-cured epoxy blanket encapsulated PSCs decreased by 8% its initial value in about 6 d, whilst PIB-packaged modules maintained excellent PCE stability for more than 200 d. The latter outcome further corroborated the conclusion that the stability improvements were mainly ascribable to the low elastic modulus and superior barrier properties of PIB encapsulant material, as well as to its chemical inertness with respect to PSCs (as opposed to UV-curable epoxy and EVA sealants).

Summarizing, glass-glass encapsulation with thermo-curable sealants is able to provide mechanically/thermally stable and high-quality oxygen and moisture barrier. Still, such method typically requires high-temperature (>100 °C) processing, which is not compatible with temperature-sensitive PSCs that always show a remarkable decrease of PCE after heating at the curing temperature of the sealants, mainly due to the thermal instability of HTL [54] considering that highly temperature resistant perovskite materials, such as $FAPbI_3$ and triple cation perovskites can endure temperatures in the range of 130° C–170° C without evident degradation [13, 14]. Hence, with the aim of reducing the impact of heat-sealing on the performance of PSCs, in many research works thermo-curable sealant have been replaced by UV-curable adhesives despite the higher costs of the latter.

To this end, Ramasamy *et at* [97]. reported a low temperature (<50 °C) glass-glass encapsulation of PSCs carried out using a UV-curable epoxy edge sealant (Vitralit, Panacol). During UV irradiation for 260 s, the device temperature was found to increase from 26 °C to 48 °C since the photocuring reaction is inherently an exothermic reaction [127]. For comparison, encapsulation of similar PSCs using thermo-curable Surlyn ionomer gasket was also prepared by heating the device at 125 °C for 10 min. Current-voltage characteristics of PSCs before and after encapsulation with Surlyn and UV-epoxy edge sealant proved the efficacy in the use of UV-curable adhesives (see figure 4(A)). In particular, while the PSC device encapsulated with UV-curable epoxy edge sealant was found to retain 85% of its original performance, a 25% decrease in device efficiency was observed in PSC systems packaged with Surlyn heat sealant, in agreement with previous studies [5, 84]. These outcomes highlight that the lower the processing temperature reached during curing step, the smaller the drop in PCE of PSCs with respect the original value. The reduced, but non negligible decrease in the performance of PSCs encapsulated with UV-curable epoxy edge sealant could mainly be related to the degradation of the mesoporous TiO_2 electron transport layer under UV illumination, that generates non-stoichiometry induced defects and gives rise to trap-assisted recombination of the photo-generated electrons in the TiO_2-based ETL [56]. Preliminary stability studies on both the devices under moderate stress conditions, that is by storing the devices in the dark at 30 °C—50% RH and periodically measuring the PV performance under 1 sun illumination, were performed. As depicted in figure 4(B), Devices encapsulated with Surlyn maintained 60% of their initial performance after 70 d of aging, whereas those encapsulated with UV-epoxy exhibited a similar trend but with slower degradation rate. The performance gradually decreased during the first 30 d and then stabilized at 83% of the initial performance, so that after 70 d of aging about 80% of initial efficiency was retained. These results could be ascribed to the superior barrier properties (i.e. WVTR, adhesion, thickness) of UV-cured epoxy adhesive that allow the UV-cured epoxy edge sealing to more effectively prevent moisture ingress with respect to Surlyn sealant. However, most epoxies are rigid and crack easily with temperature cycling [91].

Leijtens *et al* [56] demonstrated that UV induced instability can be overcome by substituting the mesoporous TiO_2-based ETL with a mesoporous Al_2O_3 scaffold. Contrary to the behaviour observed for TiO_2-based cells, the value of photocurrent density was found to remain stable after encapsulation (the PCE value passed from 6.2% to 5.7%) with an epoxy resin and a glass coverslip in a nitrogen-filled glove box. Also, a noticeable long-term stability under light soaking for 1000 h under 1 sun, AM1.5 illumination, at 40 °C was detected. After a 50% loss in efficiency during the first 200 h of exposure, due primarily to

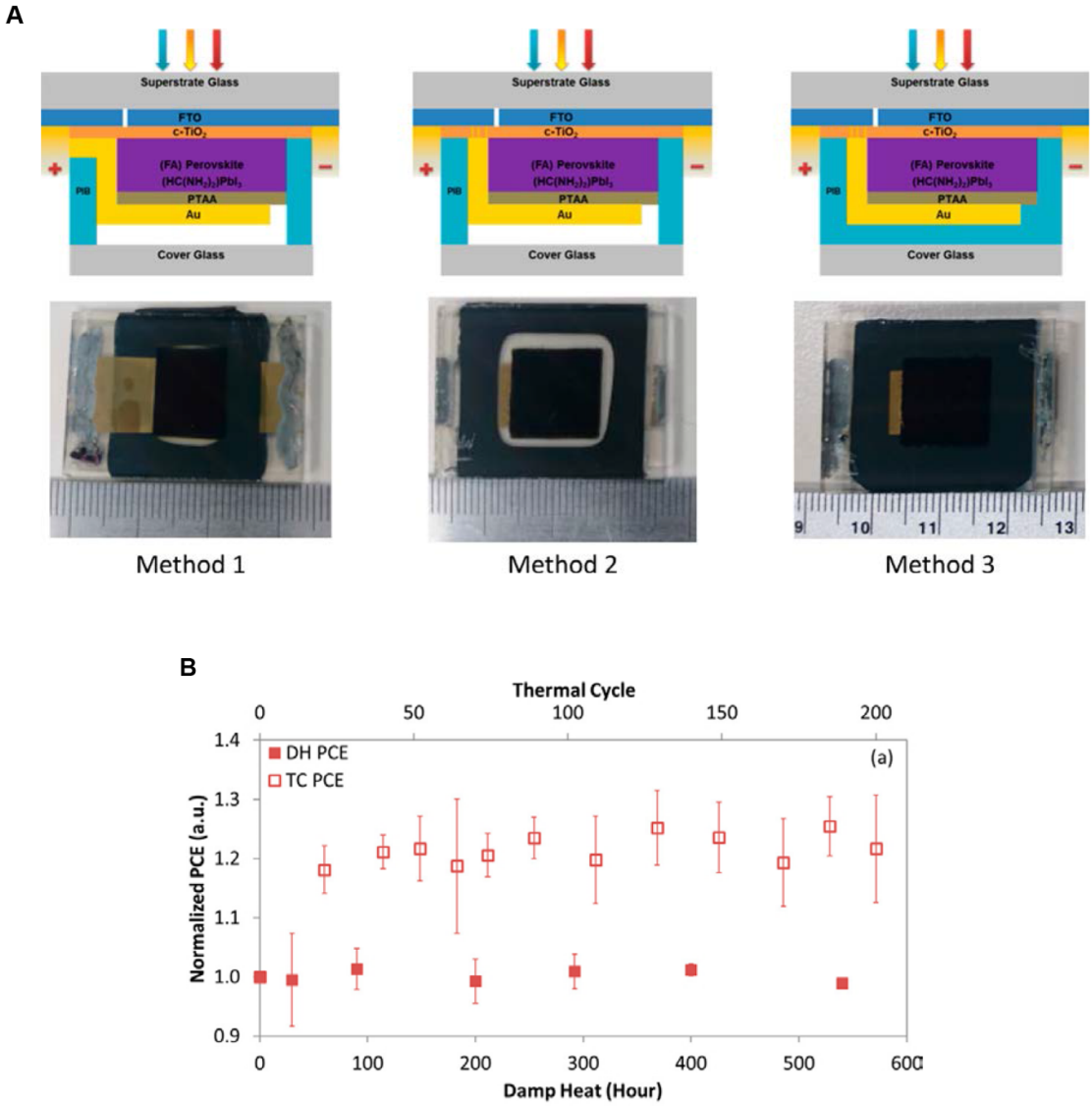

Figure 3. (A) Cross-sectional schematics and plan-view photographs from the FTO glass side of PSCs encapsulated by three methods. In method 1, PIB is applied as edge sealant over the positive electrical feedthrough for the cell. In methods 2 and 3, both electrical feedthroughs are provided by the FTO layer. But, while in methods 2 PIB is used as an edge seal only, in method 3, it acts both as edge sealant and as cover encapsulant. (B) Normalized PCE during damp heat and thermal cycling tests for PSCs encapsulated using method 3. Reprinted with permission from [85], American Chemical Society, Copyright 2017.

deterioration in the FF and V_{oc} of the cells, the efficiency remained constant. The authors pointed out that the initial efficiency drop could due to a number of factors including partial de-doping of the spiro-OMeTAD hole conductor, corrosion of silver charge colleting electrode when in contact with the perovskite layer or indeed some subtle changes within the perovskite absorber.

Alternative approaches to overcome the aforementioned issues linked to the decrease of the PV performance as a consequence of the encapsulation process include the use of an epoxy sealant curable under visible light, as recently proposed in comparison with other sealing strategies [84]. In particular, to assess the effect of the sealing procedure, after the initial characterization, PSCs were glass-glass encapsulated varying sealing material and curing strategies, and the encapsulated cells were tested again. The glass-glass encapsulation carried out with a commercially available methacrylate glue cured upon visible light using a Xenon lamp at 1 Sun intensity for 10 s allowed to limit the decrease of device performance after encapsulation (the PCE reduction was estimated being 14.3%). If compared with the value of PCE decrease for PSCs glass-glass encapsulated using a thermo-curable sealant, Surlyn 60, 32.4% drop in PCE with respect to its initial value, and a UV-curable glue, 18% decrease in PCE with respect to its initial value, a noticeably smaller reduction of PV performance was highlighted. The non-negligible performance loss still present was related to the reaction of the photoactive layers with vapours outgassing from the glue during the light-assisted curing, as previously reported by Han *et al* [41]. Accordingly, to prevent chemical components

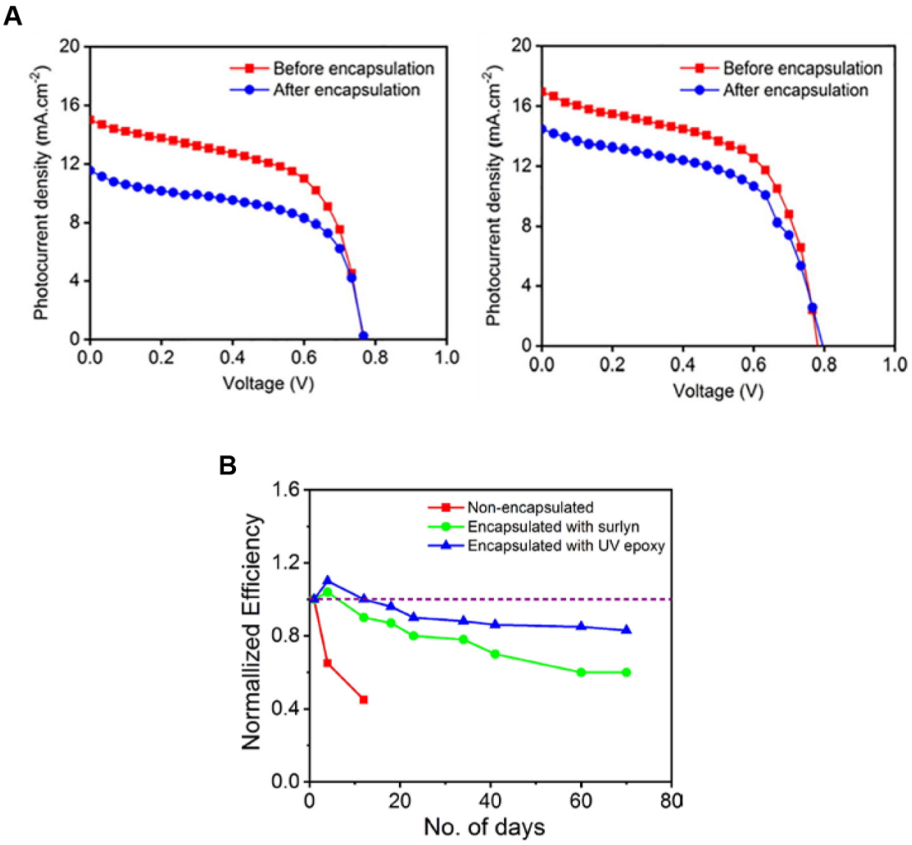

Figure 4. (A) I–V characteristics of PSCs before and after encapsulation with Surlyn (left) and UV-epoxy edge sealant (right). (B) Evolution of normalized efficiency of unencapsulated and encapsulated PSCs (with Surlyn or UV-epoxy edge sealants) stored in the dark at 30 °C, 50% RH environment. Reprinted with permission from [127], Elsevier B. V., Copyright 2019.

released by the glue during curing to affect the active layers of the PSC, a Kapton polyimide film covered with silicon-based adhesive was added in between the PSC device and the methacrylate glue. Thanks to its excellent properties in terms of chemical and temperature resistance, a minimal effect of the sealing process on the PCE of the device (reduction of only 1.5%) was observed. The effectiveness of this encapsulation procedure in the stabilization of PSC devices was further investigated under three main accelerated lifetime (ALT) tests, namely shelf-life test, damp heat test and thermal cycling stress. The shelf-life test (1500 h under dark and low humidity condition, 30% RH) yielded slightly higher PCE after 1350 h with respect to the initial PCE (3%) but 10% lower with respect to the maximum obtained after 100 h. However, when compared with devices sealed with Surlyn 60 and with UV-curable glue, in which the PCE was found to drop by 58% and 22.5% with respect to the initial value after only 170 h, respectively, the benefits of using the previously proposed sealing encapsulation protocol is evident. The damp heat test with a temperature in the range 40 °C–50 °C and 95% RH was performed to assess the lateral degradation due to the permeation of the water vapour from the edges of the device. The results of the test showed a remarkable decrease in PCE (95%) after 104 h of exposure, related to moisture-induced degradation of the perovskite layer caused by the sealing failure at the glass edges. After the application of a UV-curable epoxy glue to the edges of the encapsulated device, the performance under damp heat test strongly increased. A less pronounced PCE decrease (only 5% of the original value) was observed after 104 h. This evidence proved the importance of having an edge sealant as moisture barrier, too. Finally, to study the intrinsic effect of the temperature on the performance of the PSC encapsulated with this latter architecture (glass-glass packaged with light curable adhesive, Kapton polyimide adhesive and UV-curable edge sealant), a 250 h-long thermal test was performed at 60 °C (from 0 to 124 h) and 85 °C (from 124 h to 250 h) in an oven in dark with a relative humidity level of 25% RH (dry-heat). A linear decrease in PCE value of 0.1%/h at 60 °C and 0.21% at 85 °C was observed. This decline was mainly associated with a reduction in FF, caused by the intrinsic thermal instability of the spiro-OMeTAD layer that is subjected to partial transformation from amorphous to crystalline phase when heated [128]. On the other hand, light soaking tests induced visible intrinsic degradation of the perovskite layer. A relative reduction of PCE of 0.14%/h was found during the light-soaking test, with an absolute 20% reduction in PCE observed after 140 h. This value is remarkably lower with respect to previous reports [5], thus clearly indicating the effectiveness of this encapsulation procedure.

To further enhance the long-term stability of PSCs under high humidity conditions, a piece of desiccant [41, 129] can be placed below the cover glass with the aim of absorbing any water that may permeate through the UV resin. This combination allows to improve both the device stability under ambient conditions and in high humidity conditions (55 °C and 80% RH). Indeed, complete degradation in device performance under continuous illumination at approximately 1 sun, 55 °C and 80% RH was observed only after 120 h.

If, on one hand, a properly designed glass-glass encapsulation is still one of the strongest and most durable techniques to provide great resilience against oxygen, humidity and temperature at a low cost suitable for industrial development, on the other hand this approach only allows rigid and flat PSC modules to be operated. However, when considering the scalability of PSCs, it is important that encapsulation technologies can be compatible with the production of bendable and flexible encapsulated devices. Hence, the use of rigid substrate materials and rigid cover glass encapsulation must be avoided, and the development of alternative encapsulation strategies suitable for flexible packaged device has become essential [83, 102].

In this context, ultra-thin flexible glass encapsulation [101] and hermetic glass frit encapsulation [100, 103] have very recently gained particular interest as these emerging approaches combine excellent barrier properties and flexibility. In particular, hermetic glass frit encapsulation is a technique that not only allow to avoid the use of sealants to stack the cover glass to the device surfaces, but also enables full retention of the initial PSC module performance for 500 h under humid air exposure (80 ± 5% RH), and after 70 thermal cycles (−40 °C to 85 °C) and 50 h damp heat test (85 °C, 85% RH) according to the IEC 61215 standard. However, it requires high processing temperature (∼120 °C). Hence, more in-depth studies are currently underway with the aim of developing a similar hermetic encapsulation procedure with processing temperature lower than 85 °C to enable the use of highly efficient HTM-based devices, reducing the high fabrication costs and verifying its applicability in industrial field.

Alternatively, taking advantage from the knowledge acquired from dye sensitized solar cells (DSSCs) [130–134], organic polymer solar cells (OPVs) [70, 135, 136] and organic light emitting diodes (OLED) [137], many recent research has focused the attention on the development of polymer-based encapsulation methods to be applied in the field of PSCs. In fact, the cheapness and ready accessibility of polymer-based encapsulation techniques make them very attractive also at the industrial level.

6. Polymer-based encapsulation methods

The application of barrier films based on polymers by lamination or roll-to-roll techniques prevents the ingress of gas (i.e. water vapor or oxygen) in the device due to some important, inherent characteristics of the barrier material, including hydrophobicity, low absorption or diffusion coefficient, good adhesion.

Various commercial polymer-based barriers have been investigated as device encapsulants to shield PSCs from environmental stressors. Among these, PET [105], PTFE or Teflon [83, 106, 107], PMMA [93] and PC [80], all displaying excellent moisture- and gas-barrier properties.

Current practice in the use of polymers for encapsulation of PSCs spans from basic approaches in which EVA, Surlyn [106], UV-curable epoxy resin [138] or pressure sensitive adhesives (PSAs) [80] are combined with transparent thermoplastic foils, to more complex strategies based on thermoplastic polymeric films with integrated adhesives [83, 139], solution-processed polymeric coatings [80] and hydrophobic films [107, 140].

The use of polymer films stuck onto the PSC through an adhesive is a well-known strategy for device encapsulation owing to the intrinsic benefits such as low-cost, simple processing, and sufficient chemical stability.

Analogously to what previously highlighted when discussing glass-glass methods, one of the main limitations found in polymer-based encapsulation techniques employing thermo-curable adhesives to seal transparent thermoplastic barrier foils is the possible thermal degradation of the perovskite light harvester layer during packaging process. Consequently, encapsulation approaches relying on low-temperature lamination have been designed. Within this framework, Ramos *et al* [106] developed a two-step encapsulation process, in which the first step served as protecting layer for the following lamination step. Indeed, during the first step, a pre-encapsulation material (Surlyn 1702) was applied and cured at a low temperature (<100 °C), while in the second step proper device encapsulation was performed at higher temperatures (130 °C, during 20 min at 1 atm) by sandwiching the pre-encapsulated devices in a front/back barrier structure (Teflon 3221) using EVA as encapsulant material. This two-step method was found to be effective since a loss in PCE of only 12% was recorded.

The use thermoplastic polymeric films with integrated adhesives has also been proposed [83]. In this case, an acrylic transfer adhesive pre-coated on Kraft paper liner was used as the sealing material and it was firstly laminated onto a 240 mm commercial plastic barrier encapsulant characterized by WVTR of 5×10^{-3} g m^{-2} d^{-1} and transmittance as high as 89%. The barrier film with the laminated adhesive layer was then pre-conditioned and, after having removed the paper liner, it was laminated at 100 °C onto flexible

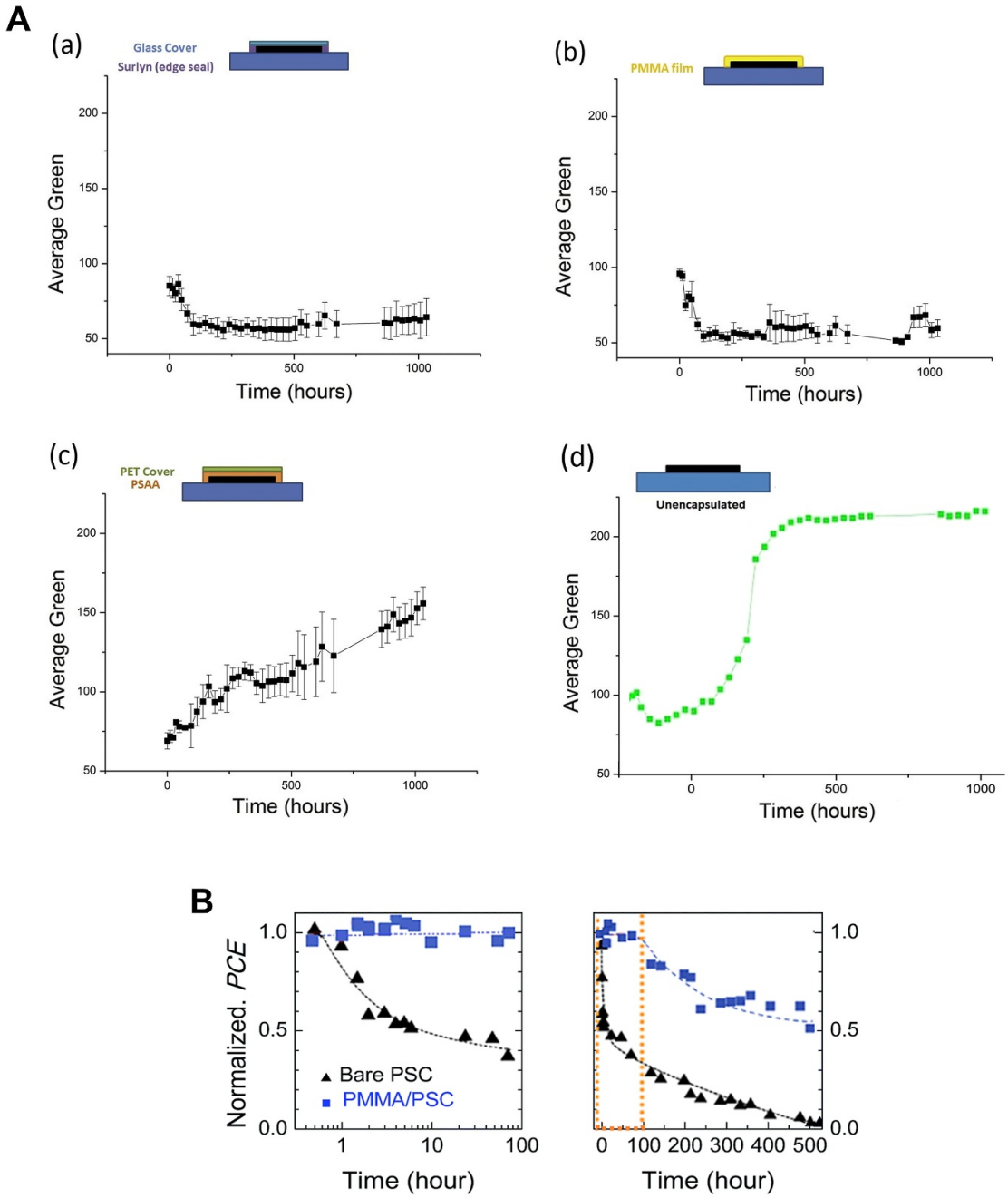

Figure 5. (A) Change in average green colour of PSCs (a) encapsulated with Surlyn + Glass cover, (b) coated with PMMA, (c) packaged with laminated PET + pressure sensitive adhesive (d) unencapsulated. Reprinted and adapted with permission from [80], Elsevier, Copyright 2016. (B) Normalized PCE as vs. storage time at RH > 75%—25 °C for (a) 100 h and (b) 500 h. Reprinted and adapted with permission from [104], Royal Society of Chemistry, Copyright 2017.

PET/IZO/TiO_2/$CH_3NH_3PbI_3$/Spiro-OMeTAD/Ag devices. In this way, no significant changes in the I–V characteristics were observed after encapsulation. Three series of devices (without encapsulation, with partial encapsulation, fully encapsulated) were investigated to assess their stability in outdoor conditions (25 °C, 30%–80% RH). This systematic research evidenced the importance of a complete device encapsulation: only completely encapsulated PSCs were able to maintain most of their initial efficiency after 500 h, whereas devices without encapsulation quickly degraded in just 100 h and devices with partial encapsulation were evidently damaged after 400 h.

A different example of polymeric film with integrated adhesive was proposed by Li *et al* [139], who employed a commercial polyimide (PI)-based Kapton tape with silicone adhesive to improve the stability of perovskite films and PSC devices. The efficacy of this facile adhesive encapsulation strategy was investigated in extreme conditions (in DI water or under thermal treatment at 240 °C). The results revealed that the encapsulated device retained its tetragonal perovskite crystal structure and its original PCE after more than

180 min at 240 °C in ambient environment and after 1800 s in DI water. The great stability of perovskite films was associated with the adhesion force established between the PI film and the perovskite film, which led to the formation of a closed system, able not only to retard the diffusion kinetics of water molecules into the perovskite structure, but also to eliminate potential diffusion paths for the volatilization of the organic component in order to enhance the thermal stability of the perovskite material.

Another possibility to avoid issues related to performance degradation during lamination and roll-to-roll processing involves the use of polymeric solution-processed layers directly spin-coated on top of the device, to cover the top surface and the edges of PSC modules [93]. In particular, encapsulation via spin-coating using commercial polymers, such as PDMS [3], PMMA or PC has been proved to provide comparable results in terms of long-term stability with respect to polymeric encapsulation through lamination. Within this context, Wilderspin *et al* [80] reported a systematic study on degradation rate of samples packaged according to three different encapsulation techniques: glass-glass encapsulation with Surlyn thermo-curable sealant, polymer encapsulation through lamination of PET using PSA, and polymer encapsulation via spin-coating starting from a solution of PMMA in chlorobenzene. Red-green-blue colour (RGB) analysis, x-ray diffraction (XRD) and UV–Vis absorption measurements performed during 1000 h exposure to ambient conditions (25 °C, 30%–40% RH) under illumination at 1 sun, demonstrated that the best long-term stability results were noticed in devices encapsulated with PMMA coating and in those packaged with Surlyn-glass cover. As illustrated in figure 5(A), RGB results evidenced that while in PMMA and glass-glass encapsulated devices no significant change in colour took place, non-encapsulated samples developed a sharp change in colour after 100 h. Instead, the PSA-based samples immediately started to linearly degrade, likely due to the interaction between the perovskite active layer and the solvent trapped in the PSA itself. The evolution with time of the XRD peak associated to PbI_2 in the four different samples confirmed the findings previously highlighted: the maximum intensity of PbI_2 peak in unencapsulated devices was five times higher than that observed in PMMA-coated samples. Interestingly, in accordance with other studies [104, 114], it was pointed out that PMMA-coated PSCs were not working, or they were found to exhibit a sharp drop in both J_{sc} and V_{oc} with respect to their initial values as a result of encapsulation. This result indicates that chlorobenzene (the solvent used for PMMA coating deposition) damages the Spiro-OMeTAD layer and decreases the PV performance during deposition. However, while the use of solution-processed PMMA encapsulants could pose some limitations in the selection of suitable HTLs, when the concentration of the PMMA solution exceeded a critical value (in this case, 30 wt% PMMA) the coating process was not found to affect significantly the PCE of PSCs [141], with only a reduction <5% with respect to the original value. Also, the PMMA-coated PSCs showed improved stability both in very humid (25 °C—RH > 75%) and in ambient conditions (35 °C and 40% RH). In high RH conditions (figure 5(B)), PSCs incorporating the PMMA passivation layer exhibited an almost constant PCE during the first 100 h of test, then their performance gradually decreased down to 50% of the initial value after 500 h exposure. In ambient conditions, PMMA-coated PSCs exhibited negligible change in PV performance for more than 500 h [104].

Alternatively, the use of HTL-free PSCs was also demonstrated to be an effective strategy to fully maintain the original PCE after solution-processed encapsulation and to produce PSC devices exhibiting long-term stability. Indeed, PMMA-coated PSCs without HTL retained about 95% of their initial efficiency after being exposed to air (25 °C and 35% RH) for 20 d [142].

Despite such encouraging results, the high WVTR (10°–10^2 $gm^{-2}d^{-1}$) and OTR (10^1–10^2 cm^3 $m^{-2}d^{-1}$) of commercial polymeric films compared with those of glass still limit their effectiveness as barrier layers [98]. In this regard, device encapsulation with polymer composite films or with solution-processed hydrophobic barrier coatings has recently gained noticeable attention since these approached can effectively inhibit water-induced degradation in PSCs.

For what concerns device encapsulation with polymer composite films, recent works [104, 108, 112, 113] proved that the use of polymer composites in which SiO_2 and/or GO fillers are dispersed in a polymeric matrix (e.g. PMMA, EVOH) effectively improves the long-term stability of encapsulated PSCs. It was claimed that the well-dispersed SiO_2 and GO fillers make the permeation path of gases and moisture through the polymer layer more tortuous, thus leading to an improvement of the barrier properties. An enhancement of two orders of magnitude in WVTR and a reduction in oxygen permeation of 64.4% were recorded in the polymer composite with respect to the pristine polymer itself. Also, the addition of GO in the polymeric matrix increased its hydrophobicity.

The notably limited stability of PSCs to moisture could be also overcome by means of a simple hydrophobic passivation process, by using a Teflon layer applied on the top of the device module via spin-coating [107]. As schematised in figure 6(A), through this hydrophobic passivation approach, water infiltration was simultaneously prevented both chemically (repulsion at the molecular level by the hydrophobicity of the fluorinated polymer) and physically (encapsulation at the macroscopic level). This

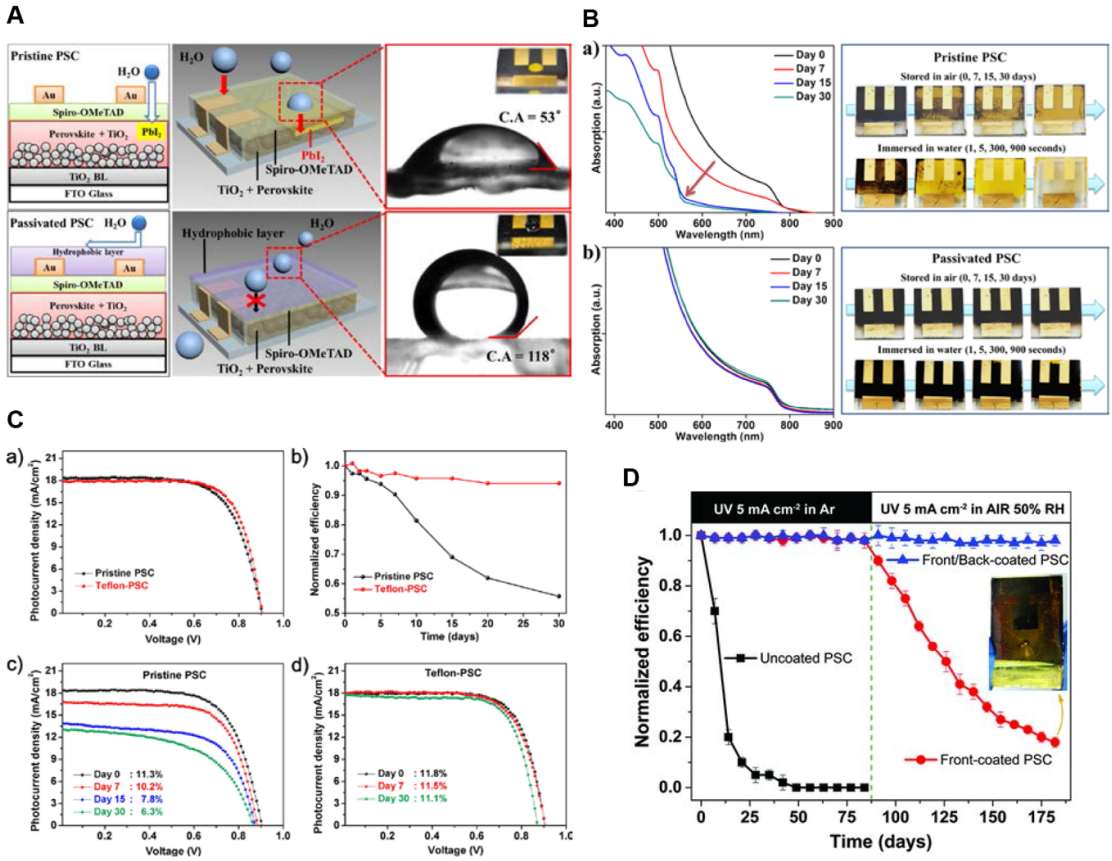

Figure 6. (A) On the left, simplified illustrations untreated cell (top) and coated (bottom) PSCs displaying the principle of hydrophobic passivation. On the right, contact angles of the untreated cell (top) and passivated cell (bottom). (B) Absorption spectrum and digital photographs of the perovskite cells, before and after storage in air ambient for 7, 15, and 30 d. On top related to untreated PSCs, while at the bottom of passivated PSCs. (C) (a) J − V curves of uncoated PSC and coated-PSC. (b) Normalized PCE of both of the PSCs. Variation of J − V curves during 30 d aging test in ambient condition on the untreated PSC (c) and passivated PSC (d). Reprinted with permission from [107], American Chemical Society, Copyright 2015. (D) Evolution of normalized PCE during aging test on the three series of PSCs: uncoated, front-coated with the luminescent fluorinated coating, and front/back-coated, obtained by coating the back contact of a front-coated PSC with the moisture-resistant fluoropolymeric layer. A digital picture of a front-coated solar cell after the test is also reported. Reprinted with permission from [140], American Association for the Advancement of Science, Copyright 2016.

resulted into a significantly enhanced stability of the PSCs both in ambient conditions and when submerged in DI water. XRD analysis, quartz crystal microbalance (QCM) measurements and UV–Vis spectra indicated that a negligible degradation occurred in the Teflon-treated PSC devices when exposed to ambient conditions (figure 6(B)). Indeed, they exhibited considerably stable performances retaining 95% of the initial PCE after 30 d (figure 6(C)). The passivated cells even showed water-repellence when submerged under water for few seconds.

Another hydrophobic barrier coating material, obtained by the combination of a UV-curable chloro-trifluoro-ethylene vinyl ether fluoropolymer binder and a dimethacrylic perfluoropolyether oligomer, was proposed by Bella *et al* [140]. They produced multifunctional luminescent downshifting fluoropolymer coatings that confer luminescent and easy-cleaning features on the front side of the devices, while concurrently forming a strongly hydrophobic barrier toward environmental moisture on the back-contact side. These photopolymers enable to absorb UV light and re-emit it in the visible range by fluorescence, preventing the UV portion of the incident solar spectrum from negatively interacting with the PSC stack and boosting the photocurrent by 6%. Additionally, they act as hydrophobic barriers, thus avoiding hydrolytic phenomena of the perovskite material and keeping the front electrode clean by means of the easy-cleaning characteristics of this fluorinated polymer. Thanks to the stabilizing effect of the fluoropolymeric coatings, the front/back-packaged PSCs retained their full functional performance (95% of their initial efficiency) even after 6 months under outdoor conditions (figure 6(D)).

These results demonstrate that polymer-based encapsulation through passivation processed using hydrophobic barrier polymers is a potentially new kind of approach to significantly enhance the stability of PSCs to moisture. However, depositing a hydrophobic layer on a hydrophilic perovskite could lead to incomplete film coverage or to the formation of overly thick films, possibly with pinholes, that could also

induce high series resistance in the PV device [143]. Moreover, most of this passivation layers exhibit high OTR values.

It is therefore important to deposit at least one metal, metal oxide or modified polymer layer on top of the polymeric barrier coating, serving as blocking or trapping layer for molecular oxygen (and water in some cases). For this reason, organic-inorganic hybrid polymer-based multilayers based on roll-to-roll deposition and thin-film encapsulation technologies based on vacuum deposition techniques are currently becoming object of increasing interest.

Organic-inorganic hybrid polymer-based multilayer flexible barriers (HPMBs) are usually composed of a first polymeric layer (e.g. PET or PEN), a second and fourth inorganic layer (typically zinc-tin-oxide, Zn_2SnO_4 (ZTO)) sandwiching a third one made of ORMOCER (organic-inorganic hybrid polymer) [109–111]. HPMBs exhibit WVTR (WVTR $\sim 1 \times 10^{-3}$) reduced by approximately three orders of magnitude if compared with PET-only protective layers. Also, a recent study [78] revealed that the barrier properties HPMBs could be further improved by a factor of 6 if the back side of the HPMB is glued over the PSC device (i.e. last ZTO layer facing the PSC module). However, some delamination and sealing issues upon application were noticed, likely indicating poor adhesion of the glue/resin with the ZTO layer of the multilayer stack. Therefore, an additional $SiO_xC_yH_z$ layer was deposited prior to the first ZTO layer to improve the poor adhesion between resin sealant and multilayer stack, thus avoiding potential sealing issues as well as further reducing WVTRs by a factor of 5 compared to barriers without $SiO_xC_yH_z$ layer. Moreover, as demonstrated from aging tests performed in dark conditions at constant room temperature and relative humidity, the long-term stability of PSCs encapsulated using HPMBs with $SiO_xC_yH_z$ as first layer not only resulted more stable with respect to the same PSCs encapsulated with a single polymeric layer, but they were also found to exhibit comparable long-term performance to glass-glass encapsulated PSCs. The low WVTR values (WVTR $= 8.2 \pm 0.3 \times 10^{-4}$) close to those of glass, the flexibility, the lightweight and the compatibility with roll-to-roll lamination processes of HPMBs make these materials highly performing, transparent encapsulation systems.

7. Thin-film encapsulation methods

Together with flexible glass and HPMBs packaging techniques, thin-film encapsulation (TFE) can be considered as one of the most interesting techniques for long-term stabilization of encapsulated PSCs. From a process perspective, deposition techniques such as CVD, PVD, PECVD, ALD, PEALD among other have been explored for TFE formation as they generally allow to deposit a great variety of organic and inorganic materials and to obtain barrier layers with extremely low values of WVTR and OTR (in the range of 10^{-4}–10^{-6} $gm^{-2}d^{-1}$ and 10^{-3}–10^{-4} cm^3 $m^{-2}d^{-1}$, respectively) [77, 102, 114, 115]. In particular, as well demonstrated in the case of direct deposition of barrier layers on temperature sensitive devices such as OLED and OPV technologies [144–149], ALD enables the fabrication of ultra-thin, highly conformable, continuous, dense and pinhole-free inorganic layers acting as moisture barriers, in a large range of deposition temperatures [62, 150].

To this end, Choi *et al* [35] recently demonstrated a promising ultrathin compact aluminum oxide Al_2O_3 layer deposited by ALD (ALD-Al_2O_3) and characterized by a WVTR value of 1.84×10^{-2} $gm^{-2}d^{-1}$ at 45 °C–100% RH. To study the effect of processing temperature on both PV properties and degradation rate of two different kinds of mesoporous perovskite devices, namely FTO/bl-TiO_2/mp-TiO_2/$(FAPbI_3)_{0.85}$ $(MAPbBr_3)_{0.15}$/HTL/Au/ALD-Al_2O_3 with spiro-OMeTAD or (poly[bis(4-phenyl)(2,4,6-trimethyl phenyl)amine]) (PTAA) as HTL, ALD-based encapsulation was repeated at three different temperatures (95, 105, 120 °C) and the PCE of the PV cells before and after ALD process was measured. To test the moisture barrier capability of 50 nm thick ALD-Al_2O_3 layer, encapsulated PSCs were exposed to 65 °C-85% RH and in inert atmosphere for 350 h and their performance was monitored. Similarly, the long-term stability of ALD-Al_2O_3 encapsulated PSCs was investigated at 25 °C-50% RH for 7500 h. First, it was demonstrated that by increasing the ALD processing temperatures a sharper drop in PCE after the ALD was observed (figure 7(A)). Furthermore, in good agreement with previous studies [55, 151], mesoporous perovskite devices with PTAA as HTL resulted to be more stable than those with spiro-OMeTAD at all the three selected ALD processing temperatures, as shown in figure 7(B) Interestingly, the PCE drop rate in both 65 °C–85% RH and 65 °C (in inert) aging conditions showed similar results. This implies the effectiveness of the 50 nm ALD-Al_2O_3 encapsulant film in the protection of PSCs from moisture infiltration. Finally, excellent durability test results for mesoporous PTAA-based devices encapsulated by means of a 50 nm thick layer of Al_2O_3 were obtained, with less than 4% reduction in PCE relative to the initial value after 7500 h (> 10 months) of exposure to 50% RH under room temperature (see figure 7(C)). Despite these encouraging results, the application of an ALD-Al_2O_3 coating at 95 °C was found to systematically lead to severe failures for spiro-OMeTAD-containing PSC devices with a 12% drop in PCE with respect to the original value for

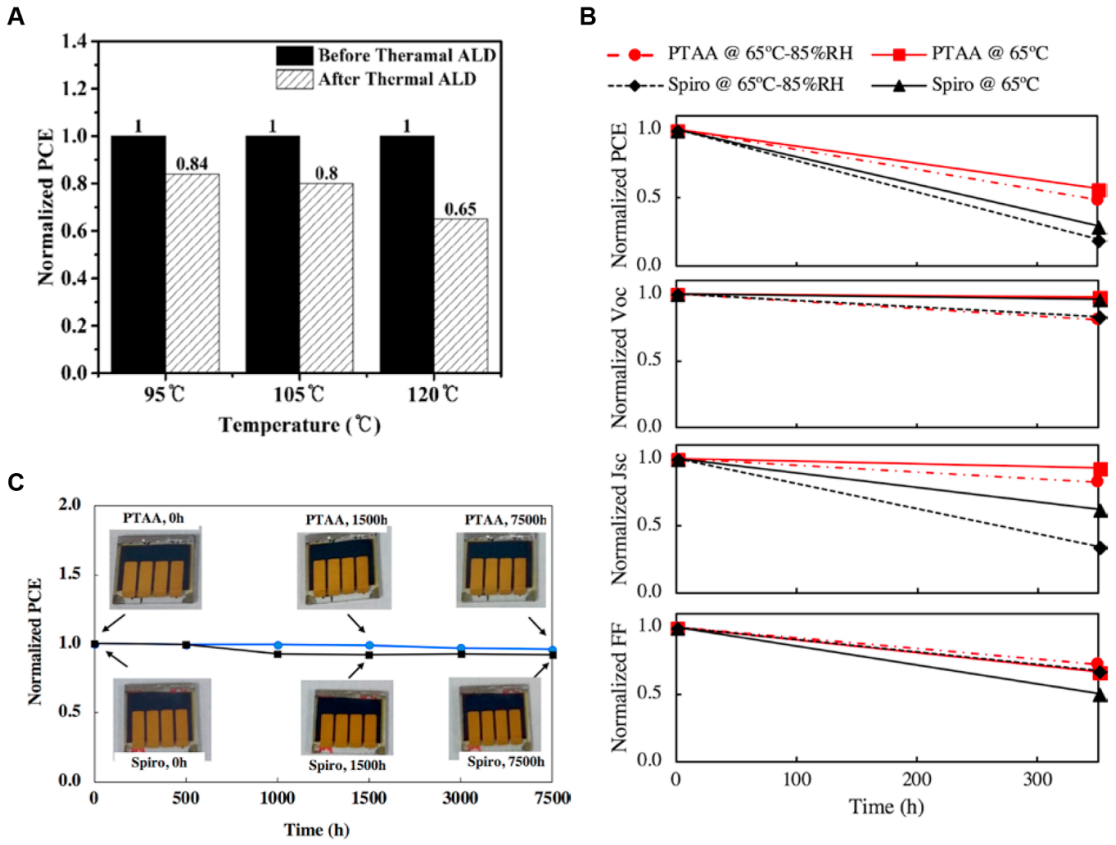

Figure 7. (A) Normalized PCE of PSCs before and after ALD of Al_2O_3 at different temperatures. (B) Normalized values of (a) PCE, (b) V_{OC}, (c) J_{SC}, and (d) FF as function of time during aging tests at 65 °C–85% RH or 65 °C (in inert) condition. Two kinds of HTL in the PSCs were tested: spiro-OMeTAD (black line) and PTAA (red line). (C) Picture and normalized PCE value of the two PSC devices (perovskite/spiro-OMeTAD/Au/ALD-Al_2O_3 and perovskite/PTAA/Au/ALD-Al_2O_3) during storage in dark at 25 °C–50% RH for 7500 h (∼ 10 months). Reprinted with permission from [35], Elsevier, Copyright 2018.

PTAA-based ones. Therefore, further development is required in the ALD process to minimize the thermal damages to the PSC device during encapsulation.

As a way to overcome problems related to the thermal instability of the PSC device during ALD deposition, a low temperature (60 °C) encapsulation process based on a single thin coating of ALD-Al_2O_3 was introduced [117, 118]. The experimental results showed that the reduction of the processing temperature to 60 °C helped to suppress such performance decline during encapsulation. In particular, ∼94% of the original PCE was retained after encapsulation of a FTO/bl-TiO_2/mp-TiO_2/$(FAPbI_3)_{0.87}(MAPbBr_3)_{0.13}$/PTAA/Au device with a 21.5 nm thick ALD-Al_2O_3 film. However, the ambient long-term stability of the devices ALD-encapsulated at 60 °C was found to be poorer compared with previous studies on similar systems [35], showing higher losses in PCE during aging (loss of ∼25% of the initial PCE after 2250 h of storage at 25 °C-50% RH). Indeed, the decreased processing temperature partly impedes the reaction between the precursor of Al_2O_3 to generate unreacted residues, which create defects in the resulting ALD-Al_2O_3 film. Therefore, the increased defect density in the encapsulation film makes it more permeable to water vapor, so that the WVTR of 60 °C-processed films presents values of one order of magnitude higher than those exhibited by 90 °C-processed films [152].

Based on these considerations, in order to avoid structural and morphological defects and pinholes intrinsically present in the fully-inorganic encapsulation film to affect its oxygen and moisture barrier properties, the insertion of an organic layer beneath the inorganic layer has been proposed as a viable approach [116, 117]. In this sense, two different strategies have been mainly adopted in the literature: one consisting in the deposition of an ultrathin compact ALD-Al_2O_3 film on an organic carrier film (e.g. the PET substrate), which is subsequently applied on top of the perovskite device; the other consisting in the direct deposition of a multilayer stack on the PSC top surface. Such multilayer thin-film encapsulation process is achieved by alternating organic and inorganic layers, where the inorganic layer is mainly responsible for the barrier performance, while the organic layer effectively elongates the torturous path of the penetrating moisture and oxygen vapours, thereby resulting in enhanced barrier properties of the overall barrier film. Also, the organic layer allows to improve the mechanical properties of the multilayer, since it enhances the

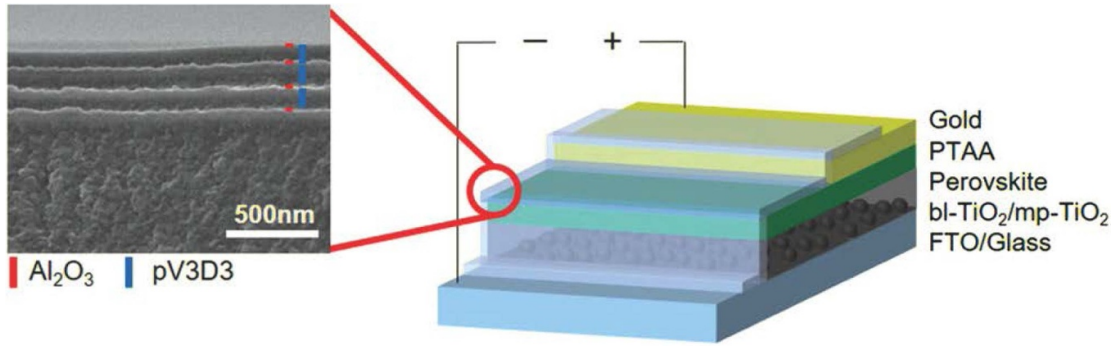

Figure 8. Schematic design of the packaged PSC (on the right), and cross-sectional SEM image of the TFE multilayer. Reprinted with permission from [117], WILEY-VCH Verlag GmbH & Co, Copyright 2017.

flexibility of the barrier film by releasing the interfacial stresses of the brittle inorganic layer, ultimately avoiding delamination [35, 153, 154].

Encapsulation by means of an ALD Al_2O_3-coated organic carrier film has been successfully applied for the first time by Chang *et al* [116] on semi-transparent PSCs. A 50 nm-thick ALD-Al_2O_3 layer was firstly deposited on a PET substrate which was then applied on top of a Ag-NW/ZnO/perovskite/PEDOT:PSS/ITO device with a UV-curable adhesive. A huge advantage of this approach is the possibility to manufacture the encapsulation stack in advance, so that production conditions are not limited by the sensible organic device and highly efficient barrier layers can be produced. However, the lamination step itself, in which the barrier film is stuck onto the device using a suitable adhesive (hot-melt, pressure sensitive or UV-curing sealants) strongly affects the original performance of the PSC. Owing to the excellent gas barrier behaviour of this multi-layer encapsulation (OTR $= 1.9 \times 10^{-3}$ cm^3 m^{-2}d^{-1}; WVTR $= 9.0 \times 10^{-4}$ gm^{-2}d^{-1}), the ambient long-term stability of the resulting encapsulated PSCs was greatly improved without compromising device performance and optical transmittance. Indeed, after being exposed to 30 °C—65% RH for more than 40 d, the encapsulated devices delivered negligible degradation in contrast to the pristine devices, which were found to be not working after only 10 d. Moreover, the flexibility of the encapsulation layer was tested by applying 1000 bending cycles at two different bending radii (13 and 5 mm). The obtained results showed that the encapsulation layer retained its low gas permeability upon bending at a radius of 13 nm, while these values were found to moderately increase (OTR $= 1.1 \times 10^{-2}$ cm^3 m^{-2}d^{-1}; WVTR $= 7.9 \times 10^{-3}$ gm^{-2}d^{-1}) as the bending radius changed to 5 mm, suggesting the potential application of TFE layers in flexible electronics.

This encapsulation strategy is highly attractive owing to its compatibility with roll-to-roll production processes. However, the application of a ALD Al_2O_3-coated PET encapsulant on an already formed device by means of adhesives poses the potential drawback of placing an organic sealant layer between the barrier and the actual device. The relatively high WVTR/OTR of organic adhesives and the presence of voids and/or pinholes at the interface between the sealant and the top surface of the PSC, provide a pathway for lateral ingress of water/oxygen, inevitably limiting the long-term adhesion of the protective layer to the device and effectively implying that the barrier properties of the encapsulation stack become largely dependent on those of the adhesive [155]. Consequently, direct deposition of the organic layer through highly conformal vacuum coating techniques can prompt further improvement in PSC lifetime, enhancing interface adhesion and avoiding the risks of delamination. In this respect, Lee *et al* [117] provided the first example of the direct incorporation of a multilayer TFE onto a PSC, by demonstrating an encapsulation system composed of four 250 nm poly(1,3,5-trimethyl-1,3,5-trivinyl cyclotrisiloxane)/20 nm ALD-Al_2O_3 dyads and characterized by outstanding barrier properties with a WVTR on the order of 8×10^{-5} gm^{-2}d^{-1} at an accelerated aging condition of 38 °C and 90% RH (figure 8). In such multilayer TFE architecture, the organic layer deposited by initiated chemical vapor deposition (iCVD) at 40 °C was found to enable to flatten the substrate surface of the solar cells to form an excellent interface with the Al_2O_3 film without physical and chemical defects on the device surface. Moreover, the organic layer was shown to act as a primary protective film for the PSC during heating, also preventing direct contact of the active materials with H_2O during the ALD process. Indeed, it was found that the encapsulation process did not degrade the device performance, while significantly enhancing its stability. The result of the shelf life test (50 °C and 50% RH for 300 h) conducted on the encapsulated PSC showed only a negligible change in PSC performance after 300 h (PCE reduction of ∼3%) and full retention of initial efficiency after over 1500 h at ambient conditions (25 °C and 50% RH).

Table 1. Summary of main reported sealants/adhesives used for glass-glass encapsulation methods.

Sealing Materials	WVTR[a] ($g\,m^{-2}\,d^{-1}$)	Optical/mechanical properties[b]	Curing Step[a]	Observations	Ref.
Ethylene vinyl acetate (EVA)	28	%T = 91% E = 10 MPa	Hot press 140 °C at 0.4 bar	Suitable for long-term reliability under light exposure. EVA is known to release acetic acid as curing, byproduct which degrades perovskite active layer. Also, the initial PCE of EVA-encapsulated PSC modules may be compromised (∼ 50% decrease in PCE after curing) by the high curing temperature needed to form EVA which lead to HTL degradation.	[12, 87]
Surlyn ionomer	0.66	%T = 93% E = 394 MPa	Hot press 100 °C at 0.4 bar	The lower curing temperature with respect to EVA reduces the impact of the sealing procedure on PSC performance (∼ 34% decrease in PCE after curing). Surlyn produces methacrylic acid during curing. Also, the higher elastic modulus leads to faster encapsulant delamination *vs.* EVA.	[5, 84, 87]
Polyisobutylene (PIB)	10^{-2}–10^{-3}	%T = 92% E = 9 MPa	Hot press 90 °C at 0.4 bar	Highly promising candidate both as cover encapsulant layer and edge sealant thanks to its excellent optical, mechanical and barrier properties. The average PCE of PSCs immediately before and after encapsulation was found not to be affected by the packaging processes. No harmful byproducts are formed during curing step.	[5, 85, 87]
Butyl rubber	10^{-2}–10^{-3}	%T = 92% E = 9 MPa	Hot press 90 °C at 0.4 bar	Similar properties to PIB. It is mainly used as a high-performing edge sealant.	[5, 12, 87]
UV-curable epoxy	0.15	%T ∼ 90% E = 15–40 MPa	UV lamp at room temperature	Smaller decrease in device performance after encapsulation than with thermo-curable sealants (∼ 85% of initial PCE is retained). The reduction could be attributed to the degradation of the mesoporous TiO_2 ETL upon UV exposure. Good optical, mechanical and barrier properties.	[84, 97]
Kapton polyimide film + Xenon-light-curable methacrylate	N/A	%T ∼ 90% E = N/A MPa	Xenon lamp at room temperature	Negligible reduction in PCE (1.5% with respect to the original value) of PSC modules after encapsulation. Only moderate effect of UV light on TiO_2 ETL degradation.	[84]

[a]As provided in the referenced works;

[b]Percent transmittance (%T, evaluated in the 400–700 nm wavelength range) is the main reference parameter to evaluate the optical properties of sealants, while the elastic modulus (E) is considered to account for their mechanical properties.

Table 2. Summary of the most effective encapsulation strategies of PSCs discussed in this work.

PSC stack structure	Encapsulation method	Encapsulant materials	WVTR ($g\,m^{-2}\,d^{-1}$)	Long-term stability	Observations	Ref.
glass/ITO/NiO/$Cs_{0.17}FA_{0.83}Pb(Br_{0.17}I_{0.83})_3$/LiF/PCBM/$SnO_2$/ZTO/ITO/Ag	Glass-glass encapsulation	EVA cover adhesive + butyl rubber edge sealant	N/A	No significant PCE decline after 1000 h damp test and 200 cycles of temperature cycling test (IEC 61215)	High mechanical and thermal barrier properties owing to the low elastic modulus of EVA and butyl rubber. Yet, under high humidity conditions (120 °C—100% RH for 20 h) degradative effects were visible.	[12]
glass/ITO/NiO/$Cs_{0.17}FA_{0.83}Pb(Br_{0.17}I_{0.83})_3$/LiF/PCBM/$SnO_2$/ITO/Ag	Glass-glass encapsulation	polyolefin 'ENLIGHT' + butyl rubber edge seal	N/A	Negligible PCE decline after 1000 h dry (25% RH) and damp (85% RH) heat tests at 85 °C (IEC 61215)	A disadvantage is the large secondary edge seal (glass coverslips are applied onto the edges too), which plays a key role in the stability results, but cannot be used in thin devices.	[87]
glass/FTO/c-TiO_2/$FAPbI_3$/PTAA/Au PSCs	Glass-glass encapsulation	PIB blanket (cover encapsulant + edge sealant)	N/A	No evident PCE reduction after 200 cycles under temperature cycling test and after 540 h damp test (IEC 61215)	Compared with PIB edge sealing, blanket encapsulation using PIB improved PSC thermal stability by preventing the escape of gaseous decomposition products and thus inhibiting perovskite and HTL decomposition reactions.	[85]
glass/FTO/TiO_2/$MAPbI_3$/spiro-OMeTAD/Au	Glass-glass encapsulation	Surlyn ionomer	N/A	58% PCE decrease after 170 h (dark, 30% RH and 25 °C) 37% PCE decrease after 200 cycles, temperature cycling test (IEC 61215)	Superior barrier properties with respect to other thermo-curable sealants; frequent delamination problems caused by the high elastic modulus of the sealant.	[5, 84]
glass/FTO/TiO_2/$MAPbI_3$/spiro-OMeTAD/Au	Glass-glass encapsulation	UV curable epoxy edge sealant	N/A	21% PCE decrease after 170 h (dark, 30% RH)	Superior barrier properties and minor encapsulation effects on initial PSC performance with respect to thermo-curable sealants. This encapsulation system shows high weathering and temperature resistance, good adhesive properties on PSCs.	[84, 97]
glass/FTO/TiO_2/$MAPbI_3$/spiro-OMeTAD/Au	Glass-glass encapsulation	Kapton polyimide cover adhesive + Xenon light curable glue edge seal and UV cure epoxy secondary (glass–glass) edge seal	N/A	No significant PCE reduction after 1500 h (dark, 30% RH and 25 °C) 22% PCE drop after 102 h of stability test at 50 °C and 95% RH 45% PCE loss after 240 h of thermal stability at 85 °C	Effective encapsulation system. At high temperature the significant drop in performance was ascribed to the damage on the HTM (spiro-OMeTAD) of the cell rather than the encapsulation failure. The presence of a secondary glass-glass edge sealing is the key element for achieving such long-term stability.	[84]

(Continued)

Table 2. (Continued).

PSC stack structure	Encapsulation method	Encapsulant materials	WVTR ($g\,m^{-2}\,d^{-1}$)	Long-term stability	Observations	Ref.
glass/FTO/c-TiO_2/mp-TiO_2/$Cs_{0.10}FA_{0.90}Pb(I_{0.83}Br_{0.17})_3$/HTL/Ag	Glass-glass encapsulation	Hermetic glass frit	$\sim 10^{-7}$	No evident PCE reduction after 200 cycles temperature cycling test (IEC 61215) and MIL-STD-883 tests	Excellent barrier properties. No need for sealant material. However, the extremely high processing temperature compromises the initial device performances. Therefore, the use of less efficient HTL-free PSCs is mandatory. Also, high packaging costs.	[100, 103]
glass/FTO/c-TiO_2/$MAPbI_3$/spiro-OMeTAD/Au	Polymer encapsulation (roll-to-roll lamination)	Surlyn 1702 as pre-encapsulant + Teflon 3221 front/back barrier structure sealed with EVA	N/A	Accelerated aging test to be performed (No results are reported in the article)	The two-step encapsulation process, in which the first step served as protecting layer for the following lamination step resulted to be effective since a loss in PCE of only 12% was recorded after packaging.	[106]
glass/FTO/c-TiO_2/mp-TiO_2/$MAPbI_3$/spiro-OMeTAD/Au	Polymer encapsulation (solution-processed)	Teflon	$\sim 10^{-1}$–10°	Initial PCE fully retained after immersion in water for 60 s 5% reduction of the initial PCE after 720 h at 25 °C, 50% RH, in dark	Hydrophobic nature of PTFE allows to reduce WVTR and achieve water contact angle as high as 118°.	[107]
IZO- PET/TiO_2/$MAPbI_3$/Spiro-OMeTAD/Au)	Polymer encapsulation (roll-to-roll lamination)	Viewbarrier® + 467 MP 3 M™ adhesive transfer tape	$\sim 10^{-3}$	400 h shelf test (25 °C, 50% RH, dark): - partial encaps., 20% drop in PCE - complete encaps., no PCE drop Ca test, moisture ingress after: - partial encaps., around 600 h - complete encaps., around 1000 h	Comparison between the long-term stability of 'partially' *vs.* 'completely' encapsulated devices evidenced the importance of avoiding side penetration of moisture.	[83]
glass/FTO/mp-TiO_2/$MAPbI_3$/spiro-OMeTAD/Au	Polymer encapsulation (solution-processed)	PMMA	$\sim 10^{\circ}$–10^{1}	95% of the initial PCE retained after exposure to air (25 °C and 35% RH) for 1000 h	Easy processability of polymeric solution-processed layers directly spin-coated on top of the device, to cover the top surface. Issue related to poor chemical stability of HTL during spin coating.	[80, 142]

(Continued)

Table 2. (Continued).

PSC stack structure	Encapsulation method	Encapsulant materials	WVTR ($g\,m^{-2}\,d^{-1}$)	Long-term stability	Observations	Ref.
glass/FTO/mp-TiO_2/$MAPbI_3$/spiro-OMeTAD/Au	Polymer composite encapsulation	PMMA SiO_2 and/or GO fillers	$\sim 10^{-2}$	No evident change in PCE after shelf test for 1000 h at 35 °C and 40% RH. Negligible PCE decline after being exposed to air with 35% RH at 90 °C for 100 h.	Well-dispersed SiO_2 and GO fillers in polymeric matrix lead to improved WVTR and OTR. Also, the addition of GO in the polymeric matrix increases its hydrophobicity.	[104]
glass/FTO/c-TiO_2/mp-TiO_2/$(FAPbI_3)_{0.85}(MAPbBr_3)_{0.15}$/spiro-OMeTAD/Au	Polymer-based encapsulation	Front side: multifunctional luminescent downshifting fluoropolymer coatings Back side: hydrophobic barrier coating	N/A	PSCs showed only 5% PCE decrease after 90 d exposure to real outdoor conditions (IEC 61215)	Front-side photopolymer enables to boost the initial PCE by 6% by luminescent downshifting. Hydrophobic nature of the polymer allows to reduce moisture ingress and keep the electrode clean by means of easy-cleaning features. Also, fluoropolymers are excellent for chemical and thermal resistance.	[140]
glass/FTO/c-TiO_2/mp-TiO_2/$(FAPbI_3)_{0.85}(MAPbBr_3)_{0.15}$/spiro-OMeTAD/Au	Polymer composite encapsulation	EVOH with SiO_2 and/or GO fillers	3.4×10^{-3}	Encapsulated devices maintained 86% of their performance under direct contact with water for 5 h.	Dispersion of SiO_2 and GO fillers leads to a two-order-of-magnitude enhancement in WVTR and a reduction in oxygen permeation by 64.4% with respect to the pristine polymer.	[108, 112]
glass/ITO/SnO_2/$MAPbI_3$/Spiro-OMeTAD/Au	Hybrid polymer-based multilayer encapsulation	$SiO_xC_yH_z$ + ZTO + ORMOCER + ZTO + PET	8.2×10^{-4}	76.6% PCE retained after 840 h shelf test at 25 °C, 50% RH and dark condition	Flexibility, lightweight and compatibility with roll-to-roll lamination processes and with large area devices. High%T ~ 90% in visible range.	[78]
glass/FTO/TiO_2/$MAPbI_3$/spiro-OMeTAD/Au	Polymer-based encapsulation	poly(p-chloro-xylylene) (Parylene-C)	N/A	No notable PCE change after 196 h at 25 °C and RH = 50%.	Parylene-C showed hydrophobic behaviour: contact angle of 121°. Its deposition process (consisting in vaporization, pyrolysis and polymerization at 20 °C) does not affect the original PCE.	[114]
glass/FTO/c-TiO_2/mp-TiO_2/$MAPbI_3$/spiro-OMeTAD/Au	Polymer-based encapsulation	Plasma-assisted vacuum deposition of adamantane (ADA) precursor	N/A	5% PCE drop after immersion in water for 60 s. Encapsulated PSC maintained 75% of its initial PCE after 24 h at 85% RH in dark.	The deposition carried out at room temperature does not affect the PV performance. High%T = 90% in visible range.	[115]

(Continued)

Table 2. (Continued).

PSC stack structure	Encapsulation method	Encapsulant materials	WVTR ($g\ m^{-2}\ d^{-1}$)	Long-term stability	Observations	Ref.
glass/FTO/bl-TiO_2/mp-TiO_2/$(FAPbI_3)_{0.85}(MAPbBr_3)_{0.15}$/HTL/Au	TFE	ALD-Al_2O_3	1.8×10^{-2} (at 45 °C-100% RH)	For deposition T = 120 °C, 4% reduction in PCE after 7500 h at 25 °C–50% RH in dark. For deposition T = 60 °C, 25% drop in PCE after 2250 h, 25 °C–50% RH in dark.	PSCs with PTAA as HTL resulted more stable than those with spiro-OMeTAD during encapsulation which requires deposition T > 60 °C. The higher the deposition T, the lower the film WVTR, but also the sharper decline in initial PCE.	[35, 117, 118]
glass/FTO/c-TiO_2/$MAPbI_3$/spiro-OMeTAD/MoO_3/Al	TFE + edge sealing	ALD-SiO_2 protective layer + UV-curable epoxy glue including a desiccant sheet	$\sim 10^{-4}$	20% decrease in PCE of the sealed cell after 48 h stability test under illumination at 85 °C–65% RH (ISOS-L2) and 11% PCE loss after 432 h outdoor aging test (ISOS-O1)	Promising and efficient encapsulation system also for large are PSCs. Further studies required to reduce the sensitivity to ambient humidity and to mitigate the high costs for ALD process.	[86]
glass/ITO/PEDOT:PSS/$MAPbI_3$/ALD-ZnO/Ag	TFE + polymer based- encapsulation	Al_2O_3-coated PET	9.0×10^{-4}	PSCs retained their initial PCEs after 1000 h at 30 °C and 65% RH. Encapsulation layer retained the original WVTR value after 1000 bending cycles with a 13 mm bending radius.	Superior optical transparency (%T > 90%), flexibility and long-term performance. Delamination of the encapsulant layer from PSC module occurs when subjected to cyclic bending.	[116]
glass/FTO/mp-TiO_2/bl-TiO_2/$MAPbI_3$/PTAA/Au	Multilayer TFE	iCVD- pV3D3/ALD-Al_2O_3	8.5×10^{-5}	97% PCE retained after 300 h shelf test at 50 °C and RH of 50%. Initial PCE completely retained after 1000 bending cycles with a 25 mm bending radius.	Outstanding optical transparency (%T > 90%) and flexibility. The direct deposition of multilayer TFE causes less than 0.3% degradation in initial PCE.	[117]

Together with other breakthrough studies in which different encapsulation techniques were employed (glass-glass [5, 41, 85, 100, 101] or polymer-based [83, 140] encapsulation), these results on multilayer TFE demonstrate some of the longest PSC shelf lifetimes achieved at such high incubation temperature.

To further improve the long-term stability of PSCs in real outdoor contexts, TFE can be easily combined with other encapsulation strategies, such as glass packaging using thermo/UV-curable sealant, as reported in a recent research study [86] in which PSCs were encapsulated with a 50 nm thick SiO_2 layer and then protected by a cover glass with a piece of desiccant sealed using a UV-curable epoxy glue. The encapsulated device maintained approximately 90% of its initial efficiency after 48 h of light soaking at 85 °C and 65% RH, while nearly fully retaining its original efficiency after 432 h in an outdoor humid environment (25 °C, 60%–70% RH and dark/light cycles).

Despite the important successes of TFE by means of ALD process, several important issues should be addressed before the wide application of this deposition technique in PSCs [117, 118, 156]. First, more advanced ALD deposition processes should be designed to deposit thin films on large area devices with enhanced accuracy to accommodate the need for industrial mass production of PSC panels. Second, the growth speed of thin films in ALD will need to be significantly enhanced while maintaining a much-needed low processing temperature, so as to increase the production rate while minimizing thermal damages to the perovskite active layer. Third, strategies to simultaneously encapsulate the device edges are required in order to ensure a hermetic sealing and avert lateral diffusion of water and oxygen. Fourth, it is urgent to minimize the process cost of TFE in order to limit its impact on the overall cost of the fully encapsulated PSC device, thus ensuring its wide applicability on the market.

8. Conclusion and outlook

In this perspective, a detailed discussion on currently available encapsulation strategies to improve the long-term stability of PSCs was presented, highlighting their main strengths and weaknesses (table 2).

Conventional glass-glass encapsulation has demonstrated to provide excellent resilience towards temperature, oxygen and humidity at a relatively low cost for stable PSCs to be competitive with other commercial PV technologies. Also, by properly selecting cover and edge sealants (e.g. light-curable adhesives or butyl rubbers) and by using desiccant material, glass-glass encapsulation has proven to prevent PSC performance deterioration during encapsulation and side-penetration of water vapor, thus ensuring effective long-term stability under ambient conditions (>1000 h) [84, 85]. However, the use of rigid glass sheets is not compatible with flexible and bendable devices. For that, alternative encapsulation techniques have been developed, namely polymer-based encapsulation and direct thin-film encapsulation. In the former, solution-processed or laminated polymer films are employed as barrier layers for PSCs. While polymer-based encapsulants can be easily spin-coated or laminated to achieve flexible PSC devices, their relatively high OTR and WVTR values limit their effectiveness in the ensuring long-term stability of encapsulated PSCs. In addition, mechanical stresses in the whole device assembly can have a stronger impact on device performance compared to glass-glass encapsulation, potentially leading in some cases to delamination. Therefore, to improve the reliability of polymer-based encapsulation, suitable high-barrier polymeric materials should be designed, characterized by excellent adhesion and mechanical compatibility with the underlying device surface. In this regard, the deposition of at least one metal, metal oxide or modified polymer layer on top of the polymer encapsulant has been demonstrated to effectively act as blocking layer for molecular oxygen and moisture. This is the rationale behind multilayer thin-film encapsulation, currently considered as the most promising encapsulation technique for PSCs and other flexible device applications. Indeed, multilayer thin films directly deposited on the devices can show improved surface adhesion, can effectively suppress volatile organics from escaping the perovskite material and may exhibit impressive resistance to moisture and oxygen ingress (WVTR and OTR below 10^{-5} $gm^{-2}d^{-1}$ and 10^{-3} cm^{-3} $m^{-2}d^{-1}$, respectively), ultimately allowing PSC stabilities of over thousands of hours in humid environments at room temperatures. However, the high process cost and the need for vacuum-based equipment for their production still strongly hamper their development in industrial scenarios. Efforts should also be made in designing direct TFE processes where the organic and inorganic layers are deposited with a combination of sufficiently low temperature and short processing time to prevent degradation of the underlying perovskite material. Additionally, to avoid side-penetration of oxygen and humidity and therefore to further improve the PSCs lifetime, a strategy to simultaneously encapsulate the edges of PSC devices is required. As a result, future studies aiming to overcome the above-mentioned challenges will be pivotally important for the commercialization and real industrial application of direct multilayer thin-film encapsulation methods. Similarly, the role of polymer composites in the field of PSC encapsulation is expected to grow in the near future driven by the possibility of synthetically designing materials with excellent barrier properties towards oxygen and moisture, while simultaneously ensuring easy processability at affordable processing costs.

We hope this perspective will become a useful reference for researchers working in the field of PSCs, stimulating further discussion and research in the area of device stabilization and encapsulation, and ultimately contributing to the success of perovskite-based materials and devices in the future PV market.

Acknowledgments

Financial support from the Italian Ministry of University and Research (MIUR) through grant PRIN2017 BOOSTER (protocol number 2017YXX8AZ) is gratefully acknowledged.

Author contributions

The manuscript was written through contributions of all authors. All authors have given approval to the final version of the manuscript.

Notes

The authors declare no competing financial interests.

ORCID iDs

Francesca Corsini https://orcid.org/0000-0002-9109-3737
Gianmarco Griffini https://orcid.org/0000-0002-9924-1722

References

[1] Chen Z, Turedi B, Alsalloum A Y, Yang C, Zheng X, Gereige I, Alsaggaf A, Mohammed O F and Bakr O M 2019 Single-crystal $MAPbI_3$ perovskite solar cells exceeding 21% power conversion efficiency *ACS Energy Lett.* **4** 1258–9
[2] Green M A, Ho-Baillie A and Snaith H J 2014 The emergence of perovskite solar cells *Nat. Photonics* **8** 506–14
[3] Liu Z, Sun B, Shi T, Tang Z and Liao G 2016 Enhanced photovoltaic performance and stability of carbon counter electrode based perovskite solar cells encapsulated by PDMS *J. Mater. Chem.* A **4** 10700–9
[4] Zhou D, Zhou T, Tian Y, Zhu X and Tu Y 2018 Perovskite-based solar cells: materials, methods, and future perspectives *J. Nanomater* **2018** 1–15
[5] Burschka J, Pellet N, Moon S J, Humphry-Baker R, Gao P, Nazeeruddin M K and Grätzel M 2013 Sequential deposition as a route to high-performance perovskite-sensitized solar cells *Nature* **499** 316–19
[6] Noh J H, Im S H, Heo J H, Mandal T N and Seok S I 2013 Chemical management for colorful, efficient, and stable inorganic-organic hybrid nanostructured solar cells *Nano Lett.* **13** 1764–9
[7] Asghar M I, Zhang J, Wang H and Lund P D 2017 Device stability of perovskite solar cells—a review *Renew. Sustain Energy Rev.* **77** 131–46
[8] Liu T *et al* 2018 Stable formamidinium-based perovskite solar cells via in situ grain encapsulation *Adv. Energy Mater.* **8** 1800232
[9] Yang Z, Chueh C C, Liang P W, Crump M, Lin F, Zhu Z and Jen A K Y 2016 Effects of formamidinium and bromide ion substitution in methylammonium lead triiodide toward high-performance perovskite solar cells *Nano Energy* **22** 328–37
[10] Yi C, Luo J, Meloni S, Boziki A, Ashari-Astani N, Grätzel C, Zakeeruddin S M, Röthlisberger U and Grätzel M 2016 Entropic stabilization of mixed A-cation ABX_3 metal halide perovskites for high performance perovskite solar cells *Energy Environ. Sci.* **9** 656–62
[11] McMeekin D P *et al* 2016 A mixed-cation lead mixed-halide perovskite absorber for tandem solar cells *Science* **351** 151–5
[12] Bush K A *et al* 2017 23.6%-efficient monolithic perovskite/Silicon tandem solar cells with improved stability *Nat. Energy* **2** 1–7
[13] Singh R, Sandhu S, Yadav H and Lee J J 2019 Stable triple-cation (Cs^+-MA^+-FA^+) perovskite powder formation under ambient conditions for hysteresis-free high-efficiency solar cells *ACS Appl. Mater. Interfaces* **11** 29941–9
[14] Yang J *et al* 2018 Comprehensive understanding of heat-induced degradation of triple-cation mixed halide perovskite for a robust solar cell *Nano Energy* **54** 218–26
[15] Matsui T, Yokoyama T, Negami T, Sekiguchi T, Saliba M, Grätzel M and Segawa H 2018 Effect of rubidium for thermal stability of triple-cation perovskite solar cells *Chem. Lett.* **47** 814–16
[16] Fu Q, Tang X, Huang B, Hu T, Tan L, Chen L and Chen Y 2018 Recent progress on the long-term stability of perovskite solar cells *Adv. Sci.* **5** 1–17
[17] Gholipour S and Saliba M 2020 Bandgap tuning and compositional exchange for lead halide perovskite materials *Characterization Techniques for Perovskite Solar Cell Materials* (Cambridge, MA: Elsevier) pp 1–22
[18] Ono L K, Juarez-Perez E J and Qi Y 2017 Progress on perovskite materials and solar cells with mixed cations and halide anions *ACS Appl. Mater. Interfaces* **9** 30197–246
[19] Jeon N J, Noh J H, Yang W S, Kim Y C, Ryu S, Seo J and Seok S I 2015 Compositional engineering of perovskite materials for high-performance solar cells *Nature* **517** 476–80
[20] Djurišić A B, Liu F, Ng A M C, Dong Q, Wong M K, Ng A and Surya C 2016 Stability issues of the next generation solar cells *Phys. Status Solidi. - Rapid Res. Lett.* **10** 281–99
[21] Gu F, Zhao Z, Wang C, Rao H, Zhao B, Liu Z, Bian Z and Huang C 2019 Lead-free tin-based perovskite solar cells: strategies toward high performance *Sol. RRL* **3** 1900213

[22] Park N 2019 Research direction toward scalable, stable, and high efficiency perovskite solar cells *Adv. Energy Mater.* **10** 1903106
[23] Saliba M *et al* 2016 Cesium-containing triple cation perovskite solar cells: improved stability, reproducibility and high efficiency *Energy Environ. Sci.* **9** 1989–97
[24] Wang Z, Lin Q, Chmiel F P, Sakai N, Herz L M and Snaith H J 2017 Efficient ambient-air-stable solar cells with 2D-3D heterostructured butylammonium-caesium-formamidinium lead halide perovskites *Nat. Energy* **2** 1–10
[25] Milot R L, Sutton R J, Eperon G E, Haghighirad A A, Martinez Hardigree J, Miranda L, Snaith H J, Johnston M B and Herz L M 2016 Charge-carrier dynamics in 2D hybrid metal-halide perovskites *Nano Lett.* **16** 7001–7
[26] Arabpour Roghabadi F, Alidaei M, Mousavi S M, Ashjari T, Tehrani A S, Ahmadi V and Sadrameli S M 2019 Stability progress of perovskite solar cells dependent on the crystalline structure: from 3D ABX_3 to 2D Ruddlesden-Popper perovskite absorbers *J. Mater. Chem.* A **7** 5898–933
[27] Cheng P, Wu T, Zhang J, Li Y, Liu J, Jiang L, Mao X, Lu R F, Deng W Q and Han K 2017 $(C_6H_5C_2H_4NH_3)_2GeI_4$: a layered two-dimensional perovskite with potential for photovoltaic applications *J. Phys. Chem. Lett.* **8** 4402–6
[28] Fang H H, Yang J, Tao S, Adjokatse S, Kamminga M E, Ye J, Blake G R, Even J and Loi M A 2018 Unravelling light-induced degradation of layered perovskite crystals and design of efficient encapsulation for improved photostability *Adv. Funct. Mater.* **28** 1800305
[29] Zhou T, Wang M, Zang Z, Tang X and Fang L 2019 Two-dimensional lead-free hybrid halide perovskite using superatom anions with tunable electronic properties *Sol. Energy Mater. Sol. Cells* **191** 33–38
[30] Hong K, Van Le Q, Kim S Y and Jang H W 2018 Low-dimensional halide perovskites: review and issues *J. Mater. Chem.* C **6** 2189–209
[31] Yan J, Qiu W, Wu G, Heremans P and Chen H 2018 Recent progress in 2D/quasi-2D layered metal halide perovskites for solar cells *J. Mater. Chem.* A **6** 11063–77
[32] Almutlaq J, Yin J, Mohammed O F and Bakr O M 2018 The benefit and challenges of zero-dimensional perovskites *J. Phys. Chem. Lett.* **9** 4131–8
[33] Qiu L, Ono L K and Qi Y 2018 Advances and challenges to the commercialization of organic–inorganic halide perovskite solar cell technology *Mater. Today Energy* **7** 169–89
[34] Snaith H J 2018 Present status and future prospects of perovskite photovoltaics *Nat. Mater.* **17** 372–6
[35] Choi E Y, Kim J, Lim S, Han E, Ho-Baillie A W Y and Park N 2018 Enhancing stability for organic-inorganic perovskite solar cells by atomic layer deposited Al_2O_3 encapsulation *Sol. Energy Mater. Sol. Cells* **188** 37–45
[36] Luo D, Su R, Zhang W, Gong Q and Zhu R 2020 Minimizing non-radiative recombination losses in perovskite solar cells *Nat. Rev. Mater.* **5** 44–60
[37] Kojima A, Teshima K, Shirai Y and Miyasaka T 2009 Organometal halide perovskites as visible-light sensitizers for photovoltaic cells *J. Am. Chem. Soc.* **131** 6050–1
[38] NREL 2020 National center for photovoltaics (Research cell record efficiency chart), Best Research-cell Efficiencies (https://www.nrel.gov/pv)
[39] Tai Q, Tang K-C and Yan F 2019 Recent progress of inorganic perovskite solar cells *Energy Environ. Sci.* **12** 2375–405
[40] Niu G, Guo X and Wang L 2015 Review of recent progress in chemical stability of perovskite solar cells *J. Mater. Chem.* A **3** 8970–80
[41] Han Y, Meyer S, Dkhissi Y, Weber K, Pringle J M, Bach U, Spiccia L and Cheng Y-B 2015 Degradation observations of encapsulated planar $CH_3NH_3PbI_3$ perovskite solar cells at high temperatures and humidity *J. Mater. Chem.* A **3** 8139–47
[42] Correa-Baena J-P, Saliba M, Buonassisi T, Grätzel M, Abate A, Tress W and Hagfeldt A 2017 Promises and challenges of perovskite solar cells *Science* **358** 739–44
[43] Li B, Li Y, Zheng C, Gao D and Huang W 2016 Advancements in the stability of perovskite solar cells: degradation mechanisms and improvement approaches *RSC Adv.* **6** 38079–91
[44] Vincent B R, Robertson K N, Stanley Cameron T and Knop O 1987 Alkylammonium lead halides. Part 1. Isolated PbI_6^{4-} ions in $(CH_3NH_3)_4Pb_{16}{}^*2H_2$ *Can. J. Chem.* **65** 1042–6
[45] Leguy A M A *et al* 2015 Reversible hydration of $CH_3NH_3PbI_3$ in films, single crystals, and solar cells *Chem. Mater.* **27** 3397–407
[46] Leijtens T, Bush K, Cheacharoen R, Beal R, Bowring A and McGehee M D 2017 Towards enabling stable lead halide perovskite solar cells; Interplay between structural, environmental, and thermal stability *J. Mater. Chem.* A **5** 11483–500
[47] Frost J M, Butler K T, Brivio F, Hendon C H, Van Schilfgaarde M and Walsh A 2014 Atomistic origins of high-performance in hybrid halide perovskite solar cells *Nano Lett.* **14** 2584–90
[48] Aristidou N, Sanchez-Molina I, Chotchuangchutchaval T, Brown M, Martinez L, Rath T and Haque S A 2015 The role of oxygen in the degradation of methylammonium lead trihalide perovskite photoactive layers *Angew. Chemie. - Int. Ed.* **54** 8208–12
[49] Senocrate A, Acartürk T, Kim G Y, Merkle R, Starke U, Grätzel M and Maier J 2018 Interaction of oxygen with halide perovskites *J. Mater. Chem.* A **6** 10847–55
[50] Dualeh A, Gao P, Seok S I, Nazeeruddin M K and Grätzel M 2014 Thermal behavior of methylammonium lead-trihalide perovskite photovoltaic light harvesters *Chem. Mater.* **26** 6160–4
[51] Supasai T, Rujisamphan N, Ullrich K, Chemseddine A and Dittrich T 2013 Formation of a passivating $CH_3NH_3PbI_3/PbI_2$ interface during moderate heating of $CH_3NH_3PbI_3$ layers *Appl. Phys. Lett.* **103** 1–4
[52] Conings B *et al* 2015 Intrinsic thermal instability of methylammonium lead trihalide perovskite *Adv. Energy Mater.* **5** 1–8
[53] Gunasekaran R K, Chinnadurai D, Selvaraj A R, Rajendiran R, Senthil K and Prabakar K 2018 Revealing the self-degradation mechanisms in methylammonium lead iodide perovskites in dark and vacuum *Chem. Phys. Chem.* **19** 1507–13
[54] Jena A K, Numata Y, Ikegami M and Miyasaka T 2018 Role of spiro-OMeTAD in performance deterioration of perovskite solar cells at high temperature and reuse of the perovskite films to avoid Pb-waste *J. Mater. Chem.* A **6** 2219–30
[55] Mesquita I, Andrade L and Mendes A 2019 Temperature impact on perovskite solar cells under operation *Chem. Sus. Chem.* **12** 2186–94
[56] Leijtens T, Eperon G E, Pathak S, Abate A, Lee M M and Snaith H J 2013 Overcoming ultraviolet light instability of sensitized TiO_2 with meso-superstructured organometal tri-halide perovskite solar cells *Nat. Commun.* **4** 1–8
[57] Kim H S, Seo J Y and Park N G 2016 Material and device stability in perovskite solar cells *Chem. Sus. Chem.* **9** 2528–40
[58] Kulbak M, Gupta S, Kedem N, Levine I, Bendikov T, Hodes G and Cahen D 2016 Caesium enhances long-term stability of lead bromide perovskite-based solar cells *J. Phys. Chem. Lett.* **7** 167–72

[59] Saidaminov M I, Mohammed O F and Bakr O M 2017 Low-dimensional-networked metal halide perovskites: the next big thing *ACS Energy Lett.* **2** 889–96
[60] Liao Y *et al* 2017 Highly oriented low-dimensional tin halide perovskites with enhanced stability and photovoltaic performance *J. Am. Chem. Soc.* **139** 6693–9
[61] Li Z, Klein T R, Kim D H, Yang M, Berry J J, Van Hest M F A M and Zhu K 2018 Scalable fabrication of perovskite solar cells *Nat. Rev. Mater.* **3** 1–20
[62] Zardetto V, Williams B L, Perrotta A, Di Giacomo F, Verheijen M A, Andriessen R, Kessels W M M and Creatore M 2017 Atomic layer deposition for perovskite solar cells: research status, opportunities and challenges *Sustain Energy Fuels* **1** 30–55
[63] Correa-Baena J P, Abate A, Saliba M, Tress W, Jesper Jacobsson T, Grätzel M and Hagfeldt A 2017 The rapid evolution of highly efficient perovskite solar cells *Energy Environ. Sci.* **10** 710–27
[64] Kim J H, Liang P W, Williams S T, Cho N, Chueh C C, Glaz M S, Ginger D S and Jen A K Y 2015 High-performance and environmentally stable planar heterojunction perovskite solar cells based on a solution-processed copper-doped nickel oxide hole-transporting layer *Adv. Mater. Weinheim* **27** 695–701
[65] You J *et al* 2016 Improved air stability of perovskite solar cells via solution-processed metal oxide transport layers *Nat. Nanotechnol.* **11** 75–81
[66] Grancini G *et al* 2017 One-Year stable perovskite solar cells by 2D/3D interface engineering *Nat. Commun.* **8** 1–8
[67] Niu G, Li W, Li J and Wang L 2016 Progress of interface engineering in perovskite solar cells *Sci. China Mater.* **59** 728–42
[68] Guarnera S, Abate A, Zhang W, Foster J M, Richardson G, Petrozza A and Snaith H J 2015 Improving the long-term stability of perovskite solar cells with a porous Al_2O_3 buffer layer *J. Phys. Chem. Lett.* **6** 432–7
[69] Uddin A, Upama M B, Yi H and Duan L 2019 Encapsulation of organic and perovskite solar cells: A review *Coatings* **9** 1–17
[70] Ahmad J, Bazaka K, Anderson L J, White R D and Jacob M V 2013 Materials and methods for encapsulation of OPV: a review *Renew. Sustain Energy Rev.* **27** 104–17
[71] Pern F J and Glick S H 1997 Improved photostability of NREL-developed EVA pottant formulations for PV module encapsulation *1997 26th IEEE Photovolt Spec Conf.* (Anaheim, CA: IEEE) pp 1089–92
[72] Peike C, Hädrich I, Weiß K-A and Dürr I 2013 Overview of PV module encapsulation materials *Photovolt. Int.* **19** 85–92
[73] Kovrov A, Helgesen M, Boeffel C, Kröpke S and Søndergaard R R 2020 Novel acrylic monomers for organic photovoltaics encapsulation *Sol. Energy Mater. Sol. Cells* **204** 1–9
[74] Yang J, Min M, Yoon Y, Kim W J, Kim S and Lee H 2016 Impermeable flexible liquid barrier film for encapsulation of DSSC metal electrodes *Sci. Rep.* **6** 27422
[75] Weerasinghe H C, Vak D, Robotham B, Fell C J, Jones D and Scully A D 2016 New barrier encapsulation and lifetime assessment of printed organic photovoltaic modules *Sol. Energy Mater. Sol. Cells* **155** 108–16
[76] Griffini G and Turri S 2016 Polymeric materials for long-term durability of photovoltaic systems *J. Appl. Polym. Sci.* **133** 1–16
[77] Cros S, De Bettignies R, Berson S, Bailly S, Maisse P, Lemaitre N and Guillerez S 2011 Definition of encapsulation barrier requirements: a method applied to organic solar cells *Sol. Energy Mater. Sol. Cells* **95** S65–9
[78] Castro-Hermosa S, Top M, Dagar J, Fahlteich J and Brown T M 2019 Quantifying performance of permeation barrier–encapsulation systems for flexible and glass-based electronics and their application to perovskite solar cells *Adv. Electron. Mater.* **5** 1–11
[79] Berghold J, Koch S, Frohmann B, Hacke P and Grunow P 2014 Properties of encapsulation materials and their relevance for recent field failures *2014 IEEE 40th Photovolt Spec Conf.* (Denver, CO: IEEE) pp 1987–92
[80] Wilderspin T J, De Rossi F and Watson T M 2016 A simple method to evaluate the effectiveness of encapsulation materials for perovskite solar cells *Sol. Energy* **139** 426–32
[81] Matteocci F, Razza S, Di Giacomo F, Casaluci S, Mincuzzi G, Brown T M, D'Epifanio A, Licoccia S and Di Carlo A 2014 Solid-state solar modules based on mesoscopic organometal halide perovskite: a route towards the up-scaling process *Phys. Chem. Chem. Phys.* **16** 3918–23
[82] Cheacharoen R, Boyd C C, Burkhard G F, Leijtens T, Raiford J A, Bush K A, Bent S F and McGehee M D 2018 Encapsulating perovskite solar cells to withstand damp heat and thermal cycling *Sustain Energy Fuels* **2** 2398–406
[83] Weerasinghe H C, Dkhissi Y, Scully A D, Caruso R A and Cheng Y B 2015 Encapsulation for improving the lifetime of flexible perovskite solar cells *Nano Energy* **18** 118–25
[84] Matteocci F, Cinà L, Lamanna E, Cacovich S, Divitini G, Midgley P A, Ducati C and Di Carlo A 2016 Encapsulation for long-term stability enhancement of perovskite solar cells *Nano Energy* **30** 162–72
[85] Shi L *et al* 2017 Accelerated lifetime testing of organic-inorganic perovskite solar cells encapsulated by polyisobutylene *ACS Appl. Mater. Interfaces* **9** 25073–81
[86] Dong Q, Liu F, Wong M K, Tam H W, Djurišić A B, Ng A, Surya C, Chan W K and Ng A M C 2016 Encapsulation of perovskite solar cells for high humidity conditions *Chem. Sus. Chem.* **9** 2597–603
[87] Cheacharoen R, Rolston N, Harwood D, Bush K A, Dauskardt R H and McGehee M D 2018 Design and understanding of encapsulated perovskite solar cells to withstand temperature cycling *Energy Environ. Sci.* **11** 144–50
[88] Holzhey P and Saliba M 2018 A full overview of international standards assessing the long-term stability of perovskite solar cells *J. Mater. Chem.* A **6** 21794–808
[89] Khenkin M V *et al* 2020 Consensus statement for stability assessment and reporting for perovskite photovoltaics based on ISOS procedures *Nat. Energy* **5** 35–49
[90] IEC 61215–1:2016 Terrestrial photovoltaic (PV) modules - design qualification and type approval - Part 1: test requirements (IEC) 2016 (https://webstore.iec.ch/publication/24312)
[91] Kempe M D, Dameron A A, Moricone T J and Reese M O 2010 Evaluation and modeling of edge-seal materials for photovoltaic applications *2010 35th IEEE Photovolt Spec Conf.* (Honolulu, HI: IEEE) pp 256–61
[92] Adams J *et al* 2015 Water ingress in encapsulated inverted organic solar cells: correlating infrared imaging and photovoltaic performance *Adv. Energy Mater.* **5** 1–11
[93] Mckenna B, Troughton J R and Evans R C 2017 Enhancing the stability of organolead halide perovskite films through polymer encapsulation *RSC Adv.* **7** 32942–51
[94] Watson T, Reynolds G, Wragg D, Williams G and Worsley D 2013 Corrosion monitoring of flexible metallic substrates for dye-sensitized solar cells *Int. J. Photoenergy* **2013** 1–8
[95] Liu H, Feng J, Nicoli E, López L, Kauffmann K, Yang K and Ramesh N 2012 Predicting the reliability of polyisobutylene seal for photovoltaic application *Proc. SPIE* **8472** 84720Y

[96] Strachala D, Kratochvíl M, Hylský J, Gajdoš A, Chladil L, Vaňk J *et al* 2020 Development of stable perovskite solar cell *Renewable Energy Sources: Engineering, Technology, Innovation* (Berlin: Springer) pp 653–65
[97] Ramasamy E, Karthikeyan V, Rameshkumar K and Veerappan G 2019 Glass-to-glass encapsulation with ultraviolet light curable epoxy edge sealing for stable perovskite solar cells *Mater. Lett.* **250** 51–54
[98] Lewis J S and Weaver M S 2004 Thin-film permeation-barrier technology for flexible organic light-emitting devices *IEEE J. Sel. Top Quantum Electron.* **10** 45–57
[99] Tong G, Jia Z and Chang J 2018 Flexible hybrid electronics: review and challenges *2018 IEEE Int Symp Circuits Syst.* (Florence, IT: IEEE) pp 1–5
[100] Emami S, Martins J, Madureira R, Hernandez D, Bernardo G, Mendes J and Mendes A 2019 Development of hermetic glass frit encapsulation for perovskite solar cells *J. Phys. D: Appl. Phys.* **52** 074005
[101] Castro-Hermosa S, Lucarelli G, Top M, Fahlteich J and Brown T M 2020 Perovskite photovoltaics on roll-to-roll coated ultra-thin glass as exceptional flexible power-generator for indoors *SSRN Electronic J.* **19** 00049
[102] Li L, Zhang S, Yang Z, Berthold E E S and Chen W 2018 Recent advances of flexible perovskite solar cells *J. Energy Chem.* **27** 673–89
[103] Emami S, Martins J, Ivanou D and Mendes A 2020 Advanced hermetic encapsulation of perovskite solar cells: the route to commercialization *J. Mater. Chem.* A **8** 2654–62
[104] Han G S, Yoo J S, Yu F, Duff M L, Kang B K and Lee J K 2017 Highly stable perovskite solar cells in humid and hot environment *J. Mater. Chem.* A **5** 14733–40
[105] Castro-Hermosa S, Yadav S K, Vesce L, Guidobaldi A, Reale A, Di Carlo A and Brown T M 2017 Stability issues pertaining large area perovskite and dye-sensitized solar cells and modules *J. Phys. D: Appl. Phys.* **50** 033001
[106] Ramos F J, Cortes D, Aguirre A, Castano F J and Ahmad S 2014 Fabrication and encapsulation of perovskites sensitized solid state solar cells *2014 IEEE 40th Photovolt Spec Conf.* (Denver, CO: IEEE) pp 2584–7
[107] Hwang I, Jeong I, Lee J, Ko M J and Yong K 2015 Enhancing stability of perovskite solar cells to moisture by the facile hydrophobic passivation *Appl. Mater. Interfaces* **7** 17330–6
[108] Jang J H, Kim B J, Kim J H, Han E, Choi E Y, Ji C H, Kim K T, Kim J and Park N 2019 A novel approach for the development of moisture encapsulation poly(vinyl alcohol- co-ethylene) for perovskite solar cells *ACS Omega* **4** 9211–18
[109] De Rossi F, Mincuzzi G, Di Giacomo F, Fahlteich J, Amberg-Schwab S, Noller K and Brown T M 2016 A systematic investigation of permeation barriers for flexible dye-sensitized solar cells *Energy Technol.* **4** 1455–62
[110] Nisato G *et al* 2014 Experimental comparison of high-performance water vapor permeation measurement methods *Org. Electron.* **15** 3746–55
[111] Kim M, Kang T W, Kim S H, Jung E H, Park H H, Seo J and Lee S J 2019 Antireflective, self-cleaning and protective film by continuous sputtering of a plasma polymer on inorganic multilayer for perovskite solar cells application *Sol. Energy Mater. Sol. Cells* **191** 55–61
[112] Liu Y, Liu Y and Wei S 2010 Processing technologies of EVOH/nano-SiO_2 high-barrier packaging composites *Proc.17th IAPRI World Conf. Packaging* (Tianjin: Scientific Research Publishing) pp 269–74
[113] Li X, Bandyopadhyay P, Guo M, Kim N H and Lee J H 2018 Enhanced gas barrier and anticorrosion performance of boric acid induced cross-linked poly(vinyl alcohol-co-ethylene)/graphene oxide film *Carbon* **133** 150–61
[114] Kim H, Lee J, Kim B, Byun H R, Kim S H, Oh H M, Baik S and Jeong M S 2019 Enhanced stability of $MAPbI_3$ perovskite solar cells using poly(p-chloro-xylylene) encapsulation *Sci. Rep.* **9** 15461
[115] Idígoras J, Aparicio F J, Contreras-Bernal L, Ramos-Terrón S, Alcaire M, Sánchez-Valencia J R, Borras A, Barranco A and Anta J A 2018 Enhancing moisture and water resistance in perovskite solar cells by encapsulation with ultrathin plasma polymers *ACS Appl. Mater. Interfaces* **10** 11587–94
[116] Chang C Y, Lee K T, Huang W K, Siao H Y and Chang Y C 2015 High-performance, air-stable, low-temperature processed semitransparent perovskite solar cells enabled by atomic layer deposition *Chem. Mater.* **27** 5122–30
[117] Lee Y I, Jeon N J, Kim B J, Shim H and Yang T 2018 A low-temperature thin-film encapsulation for enhanced stability of a highly efficient perovskite solar cell *Adv. Energy Mater.* **8** 1–8
[118] Ramos F J, Maindron T, Béchu S, Rebai A, Frégnaux M, Bouttemy M, Rousset J, Schulz P and Schneider N 2018 Versatile perovskite solar cell encapsulation by low-temperature ALD-Al_2O_3 with long-term stability improvement *Sustain Energy Fuels* **2** 2468–79
[119] Wang D, Wright M, Elumalai N K and Uddin A 2016 Stability of perovskite solar cells *Sol. Energy Mater. Sol. Cells* **147** 255–75
[120] Jiang S, Wang K, Zhang H, Ding Y and Yu Q 2015 Encapsulation of PV modules using ethylene vinyl acetate copolymer as the encapsulant *Macromol. React. Eng.* **9** 522–9
[121] Kempe M D, Jorgensen G J, Terwilliger K M, McMahon T J, Kennedy C E and Borek T T 2007 Acetic acid production and glass transition concerns with ethylene-vinyl acetate used in photovoltaic devices *Sol. Energy Mater. Sol. Cells* **91** 315–29
[122] Schütze M, Junghänel M, Koentopp M B, Cwikla S, Friedrich S, Müller J W and Wawer P 2011 Laboratory study of potential induced degradation of silicon photovoltaic modules *2011 37th IEEE Photovolt Spec Conf.* (Seattle, WA: IEEE) pp 000821–6
[123] Schileo G and Grancini G 2020 Halide perovskites: current issues and new strategies to push material and device stability *J. Phys. Energy* **2** 021005
[124] Kempe M D, Panchagade D, Reese M O and Dameron A A 2015 Modeling moisture ingress through polyisobutylene- based edge-seals *Prog. Photovoltaics Res. Appl.* **23** 570–5781
[125] Kempe M 2011 Overview of scientific issues involved in selection of polymers for PV applications *2011 37th IEEE Photovolt Spec Conf.* (Seattle, WA: IEEE) pp 000085–90
[126] Boyd C C, Cheacharoen R, Leijtens T and McGehee M D 2019 Understanding degradation mechanisms and improving stability of perovskite photovoltaics *Chem. Rev.* **119** 3418–51
[127] Esposito Corcione C, Malucelli G, Frigione M and Maffezzoli A 2009 UV-curable epoxy systems containing hyperbranched polymers: kinetics investigation by photo-DSC and real-time FT-IR experiments *Polym. Test* **28** 157–64
[128] Malinauskas T, Tomkute-Luksiene D, Sens R, Daskeviciene M, Send R, Wonneberger H *et al* 2015 Enhancing thermal stability and lifetime of solid-state dye-sensitized solar cells via molecular engineering of the hole-transporting material spiro-OMeTAD *ACS Appl. Mater. Interfaces* **7** 11107–16
[129] Liu F *et al* 2016 Is excess PbI_2 beneficial for perovskite solar cell performance? *Adv. Energy Mater.* **6** 1–9

[130] Weerasinghe H C, Huang F and Cheng Y B 2013 Fabrication of flexible dye sensitized solar cells on plastic substrates *Nano Energy* **2** 174–89
[131] Bella F, Griffini G, Gerosa M, Turri S and Bongiovanni R 2015 Performance and stability improvements for dye-sensitized solar cells in the presence of luminescent coatings *J. Power Sources* **283** 195–203
[132] Guillame S M, Khalil H and Misra M 2017 Polyurethane/esterified cellulose nanocrystal composites as a transparent moisture barrier coating for encapsulation of dye sensitized solar cells *J. Appl. Polym. Sci.* **134** 45010–22
[133] Griffini G, Bella F, Nisic F, Dragonetti C, Roberto D, Levi M, Bongiovanni R and Turri S 2015 Multifunctional luminescent down-shifting fluoropolymer coatings: A straightforward strategy to improve the UV-light harvesting ability and long-term outdoor stability of organic dye-sensitized solar cells *Adv. Energy Mater.* **5** 1–9
[134] Bella F, Leftheriotis G, Griffini G, Syrrokostas G, Turri S, Grätzel M and Gerbaldi C 2016 A new design paradigm for smart windows: photocurable polymers for quasi-solid photoelectrochromic devices with excellent long-term stability under real outdoor operating conditions *Adv. Funct. Mater.* **26** 1127–37
[135] Pintossi D *et al* 2016 Luminescent downshifting by photo-induced sol-gel hybrid coatings: accessing multifunctionality on flexible organic photovoltaics via ambient temperature material processing *Adv. Electron. Mater.* **2** 1–11
[136] Hösel M, Søndergaard R R, Jørgensen M and Krebs F C 2013 Comparison of UV-curing, hotmelt, and pressure sensitive adhesive as roll-to-roll encapsulation methods for polymer solar cells *Adv. Eng. Mater.* **15** 1068–75
[137] Park M H, Kim J Y, Han T H, Kim T S, Kim H and Lee T W 2015 Flexible lamination encapsulation *Adv. Mater. Weinheim* **27** 4308–14
[138] Khadka D B, Shirai Y, Yanagida M and Miyano K 2018 Degradation of encapsulated perovskite solar cells driven by deep trap states and interfacial deterioration *J. Mater. Chem.* C **6** 162–70
[139] Li B, Wang M, Subair R, Cao G and Tian J 2018 Significant stability enhancement of perovskite solar cells by facile adhesive encapsulation *J. Phys. Chem.* C **122** 25260–7
[140] Bella F, Griffini G, Correa-Baena J P, Saracco G, Grätzel M, Hagfeldt A, Turri S and Gerbaldi C 2016 Improving efficiency and stability of perovskite solar cells with photocurable fluoropolymers *Science* **354** 203–6
[141] Kishimoto T, Suzuki A, Ueoka N and Oku T 2019 Effects of poly(methyl methacrylate) addition to perovskite photovoltaic devices *J. Ceram Soc. Japan* **127** 491–7
[142] Zhang X, Zhou Y, Li Y, Sun J, Lu X, Gao X, Gao J, Shui L, Wu S and Liu J M 2019 Efficient and carbon-based hole transport layer-free $CsPbI_2Br$ planar perovskite solar cells using PMMA modification *J. Mater. Chem.* C **7** 3852–61
[143] Kim M, Motti S G, Sorrentino R and Petrozza A 2018 Enhanced solar cell stability by hygroscopic polymer passivation of metal halide perovskite thin film *Energy Environ. Sci.* **11** 2609–19
[144] Ghosh A P, Gerenser L J, Jarman C M and Fornalik J E 2005 Thin-film encapsulation of organic light-emitting devices *Appl. Phys. Lett.* **86** 1–3
[145] Chang C Y, Chou C T, Lee Y J, Chen M J and Tsai F Y 2009 Thin-film encapsulation of polymer-based bulk-heterojunction photovoltaic cells by atomic layer deposition *Org. Electron.* **10** 1300–6
[146] Meyer J, Görrn P, Bertram F, Hamwi S, Winkler T, Johannes H H, Weimann T, Hinze P, Riedl T and Kowalsky W 2009 Al_2O_3/ZrO_2 Nanolaminates as ultrahigh gas-diffusion barriers—A strategy for reliable encapsulation of organic electronics *Adv. Mater. Weinheim* **21** 1845–9
[147] Seo S W, Chae H, Seo S J, Chung H K and Cho S M 2013 Extremely bendable thin-film encapsulation of organic light-emitting diodes *Appl. Phys. Lett.* **102** 1–5
[148] Bouzid K, Maindron T and Kanaan H 2016 Thin-film encapsulated white organic light top-emitting diodes using a $WO_3/Ag/WO_3$ cathode to enhance light out-coupling *J. Soc. Inf. Disp.* **24** 563–8
[149] Fahlteich J, Glawe A and Vacca P 2016 Encapsulation of Organic Electronics *Organic and Printed Electronics: Fundamentals and Applications* (New Delhi, NCT: Pan Stanford Publishing) pp 293–353
[150] Meng X, Wang X, Geng D, Ozgit-Akgun C, Schneider N and Elam J W 2017 Atomic layer deposition for nanomaterial synthesis and functionalization in energy technology *Mater. Horizons* **4** 133–54
[151] Kim J, Park N, Yun J S, Huang S, Green M A and Ho-Baillie A W Y 2017 An effective method of predicting perovskite solar cell lifetime–Case study on planar $CH_3NH_3PbI_3$ and $HC(NH_2)_2PbI_3$ perovskite solar cells and hole transfer materials of spiro-OMeTAD and PTAA *Sol. Energy Mater. Sol. Cells* **162** 41–46
[152] Graff G L, Williford R E and Burrows P E 2004 Mechanisms of vapor permeation through multilayer barrier films: lag time versus equilibrium permeation *J. Phys. D: Appl. Phys.* **96** 1840–9
[153] Kim B J, Kim D H, Kang S Y, Ahn S D and Im S G 2014 A thin film encapsulation layer fabricated via initiated chemical vapor deposition and atomic layer deposition *J. Appl. Polym. Sci.* **131** 40974–81
[154] Kim B J, Park H, Seong H, Lee M S, Kwon B H, Kim D H, Lee Y I, Lee H, Lee J and Im S G 2017 A single-chamber system of initiated chemical vapor deposition and atomic layer deposition for fabrication of organic/inorganic multilayer films *Adv. Eng. Mater.* **19** 1–9
[155] Michels J J, Peter M, Salem A, Van Remoortere B and Van Den Brand J 2014 A combined experimental and theoretical study on the side ingress of water into barrier adhesives for organic electronics applications *J. Mater. Chem.* C **2** 5759–68
[156] Wei Y, Deng X, Xie Z, Cai X, Liang S, Ma P, Hou Z, Cheng Z and Lin J 2017 Enhancing the stability of perovskite quantum dots by encapsulation in crosslinked polystyrene beads via a swelling–shrinking strategy toward superior water resistance *Adv. Funct. Mater.* **27** 1703535